SKB

TECHNICAL REPORT 88-07

Tectonic studies in the Lansjärv region

Herbert Henkel

Swedish Geological Survey

October 1987

SVENSK KÄRNBRÄNSLEHANTERING AB
SWEDISH NUCLEAR FUEL AND WASTE MANAGEMENT CO

BOX 5864 S-102 48 STOCKHOLM
TEL 08-665 28 00 TELEX 13108-SKB

TECTONIC STUDIES IN THE LANSJÄRV REGION

Herbert Henkel

Swedish Geological Survey

October 1987

TECTONIC STUDIES IN THE LANSJÄRV REGION

Herbert Henkel

Sveriges Geologiska Undersökning

1987-10-30

CONTENTS

ABSTRACT

This report contains the results and the analysis of ground geophysical measurements and the tectonic interpretation in the 150 x 200 km Lansjärv study area. It describes the data and methods used. The significance of strike slip fault patterns in relation to the surface morphology is discussed. The obtained results are used to suggest a tentative model for the present tectonic deformation. More data on actual deformations would however be necessary to confirm and enhance the model. The report is part of the bedrock stability programme of SKB. The major conclusions regarding the tectonic structures are:

- three regional fault systems are identified, two steep NW and N trending and a third NNE trending with gentle ESE dips,

- the steep fault systems have strike slip generated deformation patterns both in the Precambrian structures and in the surface morphology,

- the post-glacial faults of the area are part of this fault pattern and represent movements mainly on reactivated, gently dipping zones,

- several suspected late or post-glacial, fault related features are found along the steep NW and N faults.

Sites for drilling and geodetic networks for deformation measurements are suggested. Detailed background data are documented in additional 4 reports. The basic geophysical and geological datasets are documented in color plotted 1:250 000 maps. A tectonic interpretation map in the same scale has been produced by combined interpretation of magnetic, elevation, elevation relief and gravity data.

SUMMARY

The choice of the Lansjärv area for tectonic studies is based on the occurrence of about 45 km of post glacial fault scarps (PGF), good access with roads, a large amount of detailed geophysical measurements, good data coverage with magnetic and elevation data, the occurrence of several regionally extending fault systems, and favourable conditions for detailed interpretation of aeromagnetic measurements.

Great effort has been spent in compilation of existing data, collection of new data at critical locations, and an integrated interpretation. In a 150 x 200 km area centered on the Lansjärv postglacial fault scarps (PGF), digital aeromagnetic, terrain elevation and gravity data have been compiled to maps and formated for use in an image analyzing system. The bedrock geology has been digitized and compiled into maps. In an inner area located around the PGF, all previous ground geophysical measurements have been compiled to a set of interpretation maps. New data were collected regarding outcrops of bedrock close to major fault zones, levelling of highest shoreline locations and ground geophysical profiles across major fault zones for dip determinations. An integrated interpretation was made for the 150 x 200 km area using magnetic, elevation and gravity data with the image analyzing system EBBA II. Dips of larger fault zones were calculated using potential field modelling techniques.

The results from the regional study show a pattern of 3 sets of fault zones which extend outside the study area. One of these sets is the NW-SE-striking Senja-Bothnian zone which is about 80 km wide and contains up to 5 major fault zones with moderate to steep, mainly SW dips. Another is the N-S-striking Seiland-Bothnian zone which is about 40 km wide and contains up to 4 major fault zones with near vertical dips. The third is a NNE-SSW-striking set of zones with gentle SE dips.

The results from the detailed study indicate that the PGF interacts in a complex pattern with the regional fault zones. The width and dip of these zones has been determined at about 40 locations. The regional fault zones are characteristically several 100 m wide and have a distinct dip. The zones are surrounded by a several km wide area with numerous lens like blocks interpreted as displaced shear lenses.

The results are documented in a set of 8 maps (on the scale 1:250 000) of the basic data sets for the entire study area, and one tectonic interpretation map on the same scale. the detailed data and interpretations are documented in 5 reports and 6 interpretation maps on the scale 1:20 000. The regional data are available on discettes formated for the image analyzing system EBBA II.

In this report, the major results are presented and discussed in a regional context. A comparison is made with active strike slip fault patterns, which shows that the steep NW and N zones show similar patterns both on a regional and a detailed scale. The occurrence of several small angular shear lenses is tentatively interpreted as effects from ongoing movements in some of the larger fault zones. It is suggested that detailed deformation measurements are located to fault zone segments which have such shear lenses and which were involved in the PGF movements.

1 INTRODUCTION

1.1 PURPOSE OF THE PROJECT

The purpose with this study is:

- to obtain a geological-geophysical basis for an optimal location of detailed studies with deformation measurements, drill holes and excavations. Of special importance is to indicate where new fracturing has occurred in the bedrock.

- to obtain an understanding within a broader regional tectonic context for where movements and earthquakes occur today.

The study is part of the SKB project "Bedrock stability". A more detailed description of the project is made in (SKB 1986).

The following sub-projects have been performed:

1 - Compilation of existing geological and geophysical data in an

a) outer area 150 x 200 km where gravity, magnetic, terrain elevation, terrain relief and geological data are stored digitally. The maps are reproduced in a smaller scale in plates 1-5. A set of maps in two sheets 1:250 000 have been prepared from these data sets, and in

b) an inner area 20 x 45 km located around the Lansjärv PGF where existing detailed surveys are compiled in 6 map sheets 1:20 000. Report by Henkel and Wållberg (1987).

2 - Additional airphoto studies to localize outcrops along larger fault zones. Report by Sundh and Wahlroos (1987).

3 - Additional ground geophysical measurements in profiles of magnetic field, VLF and slingram anomalies across larger fault zones. Model calculations for dip determinations of fault zones. Report by Arkko and Lind (1988) and Arkko (1988).

4 - Tectonic-geological reconnaissance in the inner area. Report by Talbot (1986).

5 - Photogrammetic leveling of highest shoreline levels. Report by Sundh and Wahlroos (1988).

6 - Integrated analysis of basic data compiled in sub-project 1a. This report, plate 6, Tectonic Interpretation Map and report by Henkel (1988).

1.2 PREVIOUS STUDIES IN THE LANSJÄRV AREA

The post-glacial fault scarps at Lansjärv represent the southernmost known larger set of such scarps. Two studies have been performed in the area, the first in 1981 reported

in Lagerbäck and Witschard (1983) and Henkel et al. (1983), was made for SKB and describes the PGF system geologically and geophysically. It was concluded that the PGF interact with other structures as the fault scarp height shows steps across such structures. Most such structures are other faults and together with the PGF displayed strong VLF anomalies indicating considerable amounts of water and conducting material. The other study, financed by NFR and SKB, concentrated on problems related to the interaction with other faults, the termination or continuation of PGF movements. It is concluded that the PGF end in the vicinity of large regional scale fault zones and there interact with the numerous faults occurring in the associated km-sized shear lenses. The PGF generally cut other faults with a few exceptions. Refraction seismic profiles across the PGF scarps appear to indicate a shallow dip for several of the PGF branches. This work is reported in Henkel and Wållberg (1988).

1.3 RESULTS FROM THE NORDKALOTT PROJECT

The compilation of the Aeromagnetic Interpretation Map (Henkel 1986) in the Nordkalott project shows that the linear magnetic dislocations in the Lansjärv area are part of larger structures which extend for several 100 km. They strongly disrupt the Svecokarelian lithological pattern and could be followed under the Caledonian rock units to the coast of N Norway. Across the NW-trending set of major zones, a change in the patterns of sub-Caledonian basin formation can be seen, indicating fault activity in late Proterozoic time. The NW-striking magnetic dislocations approach the Norwegian coast where the Senja Fracture zone formed in the oceanic crust at about -58 Ma. Single magnetic markers along the NW-dislocations show displacements in both sinistral and dextral sense up to about 45 km.

Along the N-trending set of major zones, several large lithological discontinuities can be seen in the interpretation map. The most important are the termination to the east of the 60 km wide schist belt SW of Rovaniemi, the bend in the Pajala-Kolari greenstone belt and the termination to the east of the Karasjokk greenstone belt N of Kautokeino. Magnetically, the N-trending set of major fault zones terminates at the Seiland Caledonian intrusive. These features have also been recognized by Berthelsen and Marker (1986), who have named the zone Bothnian Megashear and interpret it as a repeatedly active (with reversed senses) Proterozoic shear zone.

The N-trending lineaments south of Pajala are associated with a significant change in gravity caused by a step (down to the east) of intermediate density crust. This is illustrated in a series of model calculations in Arkko (1986).

1.4 BASIC DATA USED FOR THIS STUDY

A new approach has been attempted for this study by using an image analyzing system for the combined interpretation of

aeromagnetic elevation relief data and gravity data. Now the data can be analyzed using the maximal (with respect to the measurements) spatial and functional resolution. For the aeromagnetic measurements this implies a 5 times higher functional resoltuion as compared to the previously available maps (i.e. 20 nT instead of 100). The combination of aeromagnetic and elevation data turned out to be a very efficient tool for the mapping of fault patterns. The basic data sets provided for this study have the following specifications:

type	resolution spatial (m)	functional	data provided by
aeromagnetic total field anomaly	200 x 200	20 nT	Geological Survey of Sweden and Finland
gravity	400 x 400	0.2 mgal	Geological Survey of Sweden and Finland and Swedish Land Survey
elevation	100 x 100	2 m	Swedish Land Survey
bedrock geology			Geological Survey of Sweden

A set of maps dividing the study area into two sheets on the scale 1:250 000 have been prepared for each of the data sets. The functional resolution in these maps is lower than in the orginal data sets as only about 40 color levels can be visually discriminated. The Tectonic Interpretation Map has been prepared with the image analyzing system in 50 x 50 km quadrangles and was subsequently compiled and plotted in the desired scale with an electrostatic plotter.

1.5 CONTRIBUTIONS TO THIS STUDY

Contributions to this study have been made by:

Vesa Arkko and Jonas Lind, field geophysical measurements and model calculations,
Bo Wållberg, refraction seismics and detailed ground geophysical interpretations,
Mats Wedel and Herbert Henkel, image analysis and model calculations,
Jan-Eric Wahlroos, determination of highest shore line levels,
Martin Sundh, determination of outcrops along major fault zones,
Nils Dahlberg, morphologic study of low angle fault zones,
Karin Hult and Ingemar Lindgren, preparation of aeromagnetic map,
Lars Stenberg and Sandy Larkin, preparation of gravity map,

Christian Elvehage and Pentti Kaasila, preparation of topographic relief map,
Thomas Sjöstrand and Staffan Zetterlund, preparation of geological map,
Herbert Henkel and Jan Hultström, preparation of tectonic interpretation map,
Herbert Henkel, preparation of profiles.

This multidisciplinary study has been coordinated by Herbert Henkel, who is also responsible for the scientific setting and the conclusions made. In parallel with this study, numerous contacts with other scientific institutions were made. These are:

Geological Surveys of Finland, Norway, California and Canada,
Geodetic Institute of Finland,
Geodetic Survey of Finland and Sweden,
Technical Survey of Luleå and Helsinki,
University of Uppsala and Santa Barbara,
Swedish National Defense Research Institute,
Gas and Petroleum Research Institute Canada,
Swedish Space Corporation

The results of this study have regularly been reported to the Swedish Nuclear Fuel and Waste Management Co.

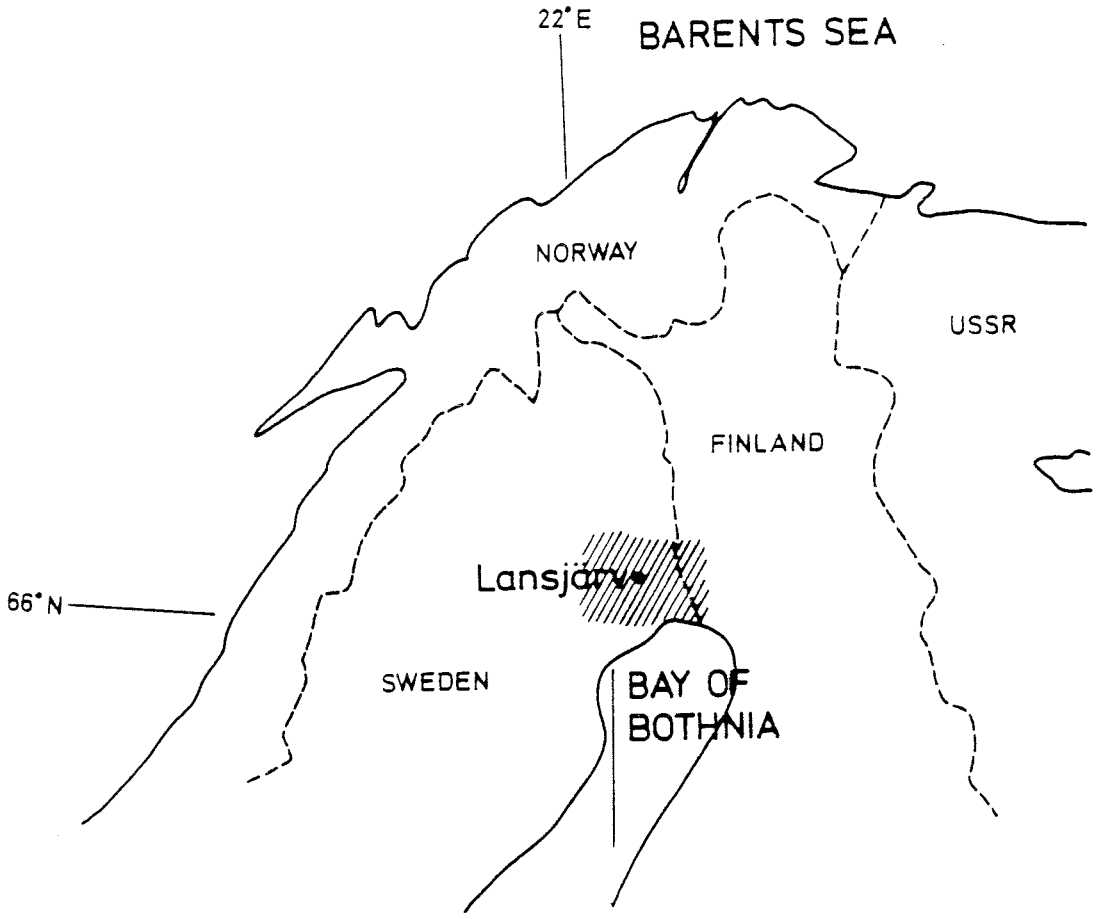

Fig. 1. Location of study area.

2. METHODS

2.1 MAGNETICS

Aeromagnetic measurements, originally made with 200 m line spacing and 30 m flight altitude, were transformed to a 200 x 200 m grid by selecting every 5th measurement along the flight lines. These data have been used to enhance and complete the study of magnetic dislocations performed in the first Lansjärv study (Henkel et al. 1983) and in the aeromagnetic interpretation map of the Nordkalott project (Henkel 1986). The following criteria were used to identify the magnetic dislocations reported here:

- linear or curved discordant magnetic minima caused by oxidation in fracture zones,
- displacements of magnetic reference structures including magnetic contacts, patterns and dykes,
- linear or curved magnetic gradients

The tendency in earlier interpretations to stress the straight aspect of lineaments has been modified to include also curved linear segments. The Lansjärv area contains numerous magnetic lithologies and structures which allow a rather detailed magnetic mapping of faults and fractures. The magnetic dislocations were digitized and entered into the image analyzing system.

Ground magnetic profiles, about 1 km long, have been measured (together with electromagnetic methods) on 34 selected minimum complexity locations across some major fault zones. These measurements were made with 20 m spaced readings to increase the spatial and functional resolution. Small scale structures cause considerable noice in some of these measurements. Both the ground and aeromagnetic measurements were used for dip calculations of major faults and fractures. These calculations are based on:

- knowledge of rock susceptibilities,
- modelling where the model anomaly is iterative brought to coincide with the measured anomaly, in several steps,
- restriction of the sense of dip using the slingram anomalies.

The network pattern of larger fault zones is very obvious. The width of single fault zones is often several 100 m. The entire fault system can be followed for several 100 km to the N and NW. An example of a set of ground geophysical profiles is shown in fig. 2. The complete documentation of all measured profiles is given in Arkko and Lind (1988).

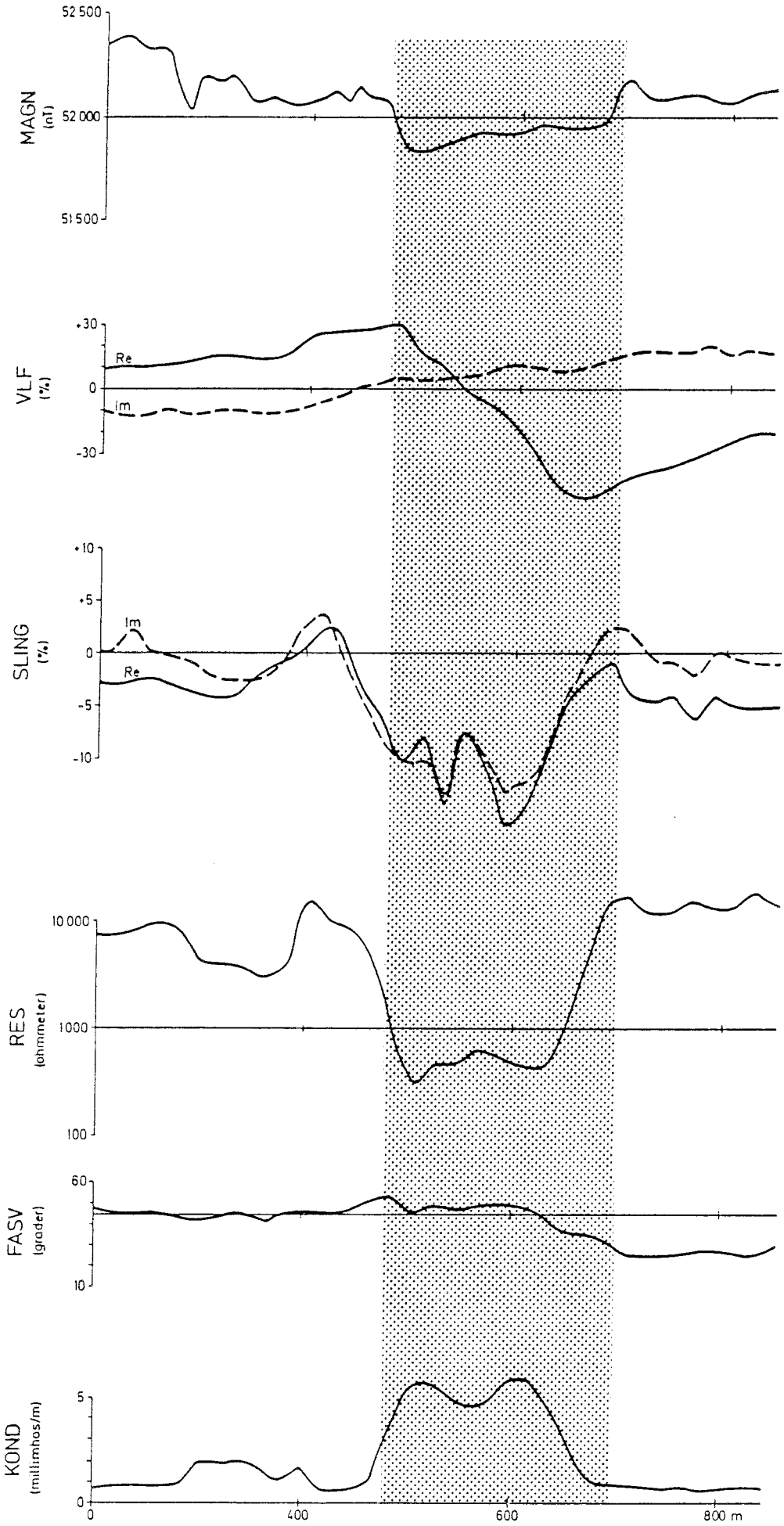

Fig. 2. Example of combined ground geophysical profile. Zone B. Profile 7.

2.2 ELECTROMAGNETICS

VLF profiles with 20 m spacing, using either the GBR or the JXZ transmitter, were made on 25 selected locations along the major fault zones. VLF anomalies arise due to conductivity changes in the uppermost 200 m of the crust. The method is very sensitive but is disturbed by power lines and telephone lines (such locations were thus avoided). In most cases the magnetic and VLF indications coincide, however the VLV method gives additional information on smaller non-oxidized faults than the magnetics. It also discriminates zones of different conductivity within the fault zone.

Slingram measurements with 100 m coil spacing, using a 16 kHz signal, were made along the same profiles as the VLF and magnetic measurements. The slingram method gives information on the location width and sense of dip of conductors in the uppermost 100 m of the crust and the soil cover. These measurements were used to constrain the magnetic model calculations. The details of within zone conductivity shown by the VLF measurements are also reflected in the slingram measurements.

In-situ resistivity measurements with the VLF method and slingram with coil spacing of 4 m provide information about the soil conductivity (by the slingram method) and the conductivity of the nearest rock units (by a combination of these two measurements). Such measurements allow more detailed studies of the width of fault zones and the nature of the uppermost rocks within them by discriminating between weathered and normal crystalline rocks.

2.3 GRAVITY

These measurements were made along roads with 1-3 km station spacing. Elevations were obtained from contoured maps in the scale 1:20 000. Gravity anomalies are caused by density contrasts associated with structures in the crust. Compared with magnetic and electromagnetic methods, only rather large structures will be visible. These include large displacements along fault zones, major unconformities and changes in crustal thickness. Gravity anomalies were used for calculations of the general dip down to about 7 km of major fault zones. In these calculations the magnetic modelling results were used as a constraint. Knowledge of rock densities is necessary for these calculations (made with the same modelling technique as for magnetics). Due to the ambiguity of the method, only limiting dips can be obtained (unless the upper surface of the buried structures can be determined independently). Combined interpretation of gravity magnetic and seismic velocity data would restrict the structural ambiguity considerably.

2.4 ELEVATION ABOVE SEA LEVEL

Coloring of topographic maps in connection with studies of meteorite impact sites has revealed the potential of tectonic

information in elevation data. The relief technique demonstrated by Elvehage (1986) has further stressed the value of digital elevation information and digital image manipulation techniques. In the Lansjärv area, 100 m spaced elevation data were accessible to the project from the Swedih Geodetic Survey. These data have an elevation resolution of about 2 m. The tectonic information reflected in the morphology is also affected by erosion and glaciation processes. Displacements of morphologic reference structures will indicate lateral movements of faults. Erosion cuts faster into the crystalline rocks where they are more fractured. Glacial processes will enhance or obliterate pre-glacial tectonic imprints depending mainly on the direction and intensity of ice flow. Post glacial tectonics will distort glacial patterns which occasionally can be seen in the elevation data. A first glance at the elevation data gives an immediate understanding of their value for tectonic interpretations. Digital image analyzing techniques can further enhance specific trends in the data. Prominent features can be sorted out from faint or sharp features. The overall impression of obvious lens shaped topographic/tectonic units indicates the importance of longtime strike slip fault movements. Also pull-apart basins and push--together ridges immediately show the effects of vertical displacements associated with strike slip movements. If an age could be assigned to the morphology, it would be possible to obtain also the rate of fault movement. Figure 3 shows with a simplistic approach how lateral fault movements can relate to graben subsidence.

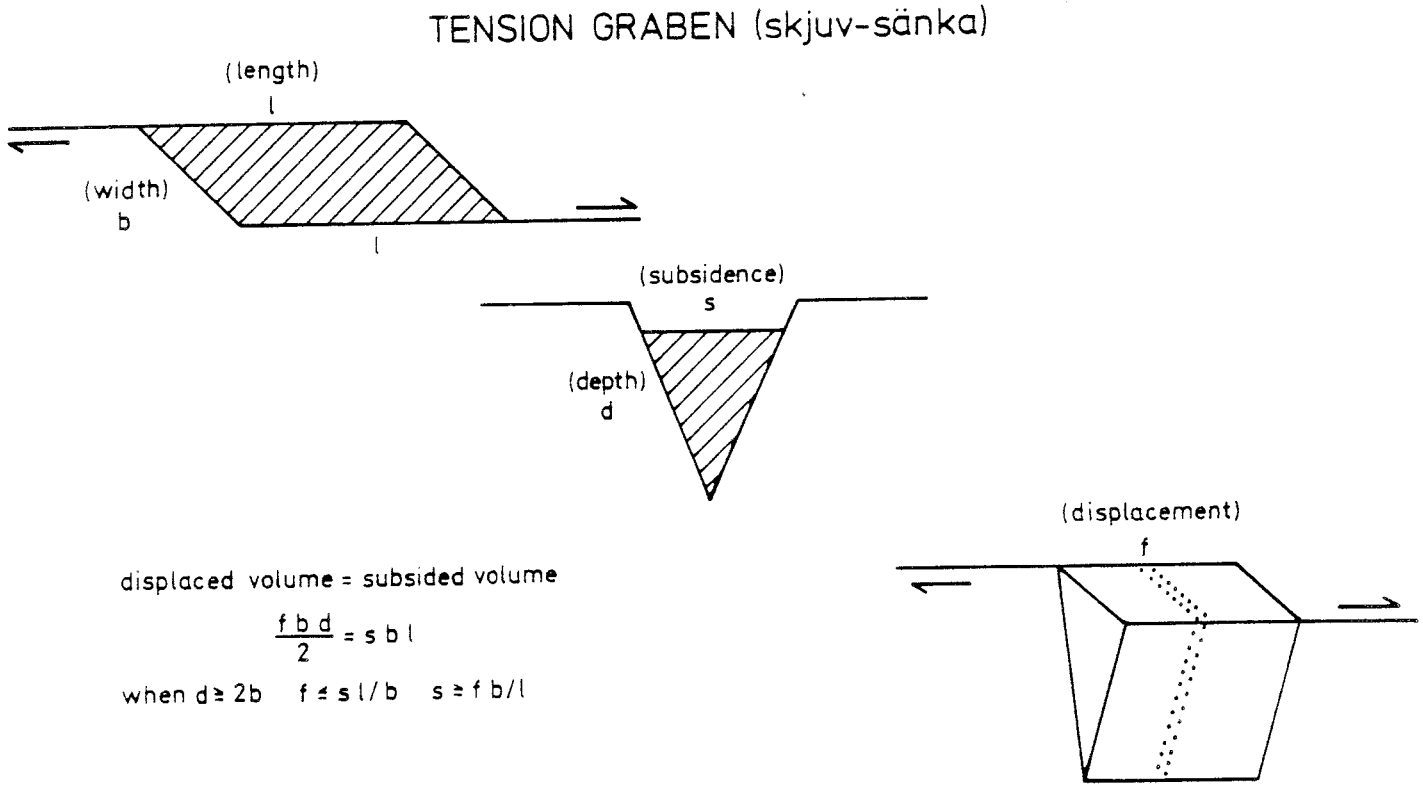

Fig. 3. Simple relation between fault displacement and subsidence in a pull-apart graben.

2.5 SEISMIC REFRACTION

The seismic refraction method (geophone spacing 5 m) has been used for the location of fracture zones, depth to the bedrock determination and mapping of PGF faults down to the bedrock. Fault zones other than the PGFs were located by using ground VLF measurements. Refraction seismics also give information about the occurrence of weathered bedrock and should therefore be used more extensively for the mapping of this reference structure. The seismic profiles are reported in Wållberg and Henkel (1987). Profiles across PGF scarps indicate that low angle thrusting may occur on most of them.

3 RESULTS

3.1 DIP AND WIDTH DETERMINATIONS OF LARGE FAULT ZONES

Figure 4 shows an example of a dip determination were magnetic measurements are used with a modelling programme. Together with the dip, also the width of the zone is obtained. All model calculations are reported in Arkko (1988). Normally a distinct anomaly is obtained when magnetic rocks are cut by an oxidized fault zone (Henkel and Guzmán 1977), or when fault movements have juxtaposed rocks with different magnetizations. In all these cases the shape of the anomaly is very sensitive to the dip of the most magnetic structure, which can be determined within 5 degrees. In ground magnetic profiles, small local structures can generate considerable noise and therefore a combination of aeromagnetic (lower noise level but less spatial resolution) and ground measurements (higher resolution of critical shape details) were used in the modelling. In the slingram measurements, an asymmetric anomaly indicates dipping sources which in many cases represents a definite constraint of the sense of dip. Also the VLF anomalies tend to develop asymmetry over dipping conductors. In those cases where the magnetic anomaly is caused by one magnetic contact only, the ground VLF resistivity constrains the width of the fault zone. This width is obtained when upper layer conductivity known from slingram measurements with small coil separation is used for the determination of the second layer (the bedrock) resistivity. A compilation of second layer resistivities found in the measured profiles is shown in figure 5.

A compilation of dip determinations is shown in figure 6. The dips of N-S-striking larger fault zones is mainly near vertical, the typical dip being 85 degrees to the east. The dips of the NW-SE-striking larger fault zones have a bimodal distribution with typical dips being 65 degrees to the NE and 60 degrees to the SW respectively. The frequencey of SW dips is higher.

Where large fault zones are also associated with distinct gravity gradients, a combined interpretation with magnetic and gravity modelling can give information about the deeper continuation of the fault zone. The gravity anomaly arises typically when large lateral displacements juxtapose structures with different densities. Figure 7 gives an example of

such a combined interpretation. As no dense rocks are known at the surface, a buried denser body must be introduced in the model, which increases the ambiguity of the result. As constraint to the fault dip, the magnetic dip determination is used in the upper 1 km of the crust. Depending on the depth to the top of the dense body, the dip for the next few km can vary between 25 degrees and the surface dip of 70 degrees. The dip cannot be steeper than the surface dip nor dip to the other direction. More calculations can be made in the area but have not been attempted at this stage of the work.

Notice that the faulted edge of the higher density structure is obtained by strike-slip motion.

In figures 8 and 9 the modelled dips and width are shown with their locations. Further dip determinations can be made at many places.

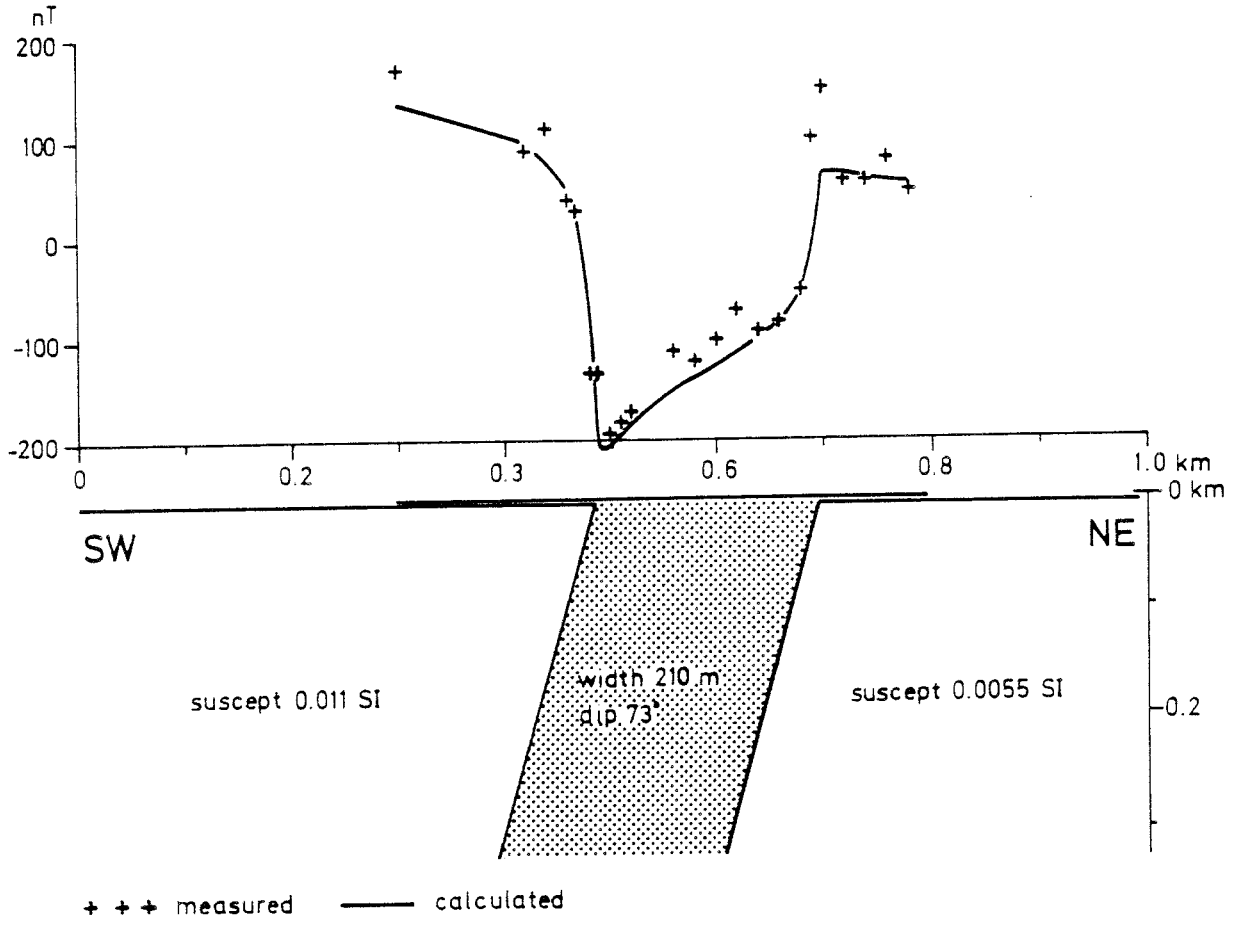

Fig. 4. Magnetic model calculation of NW zone at profile 7.

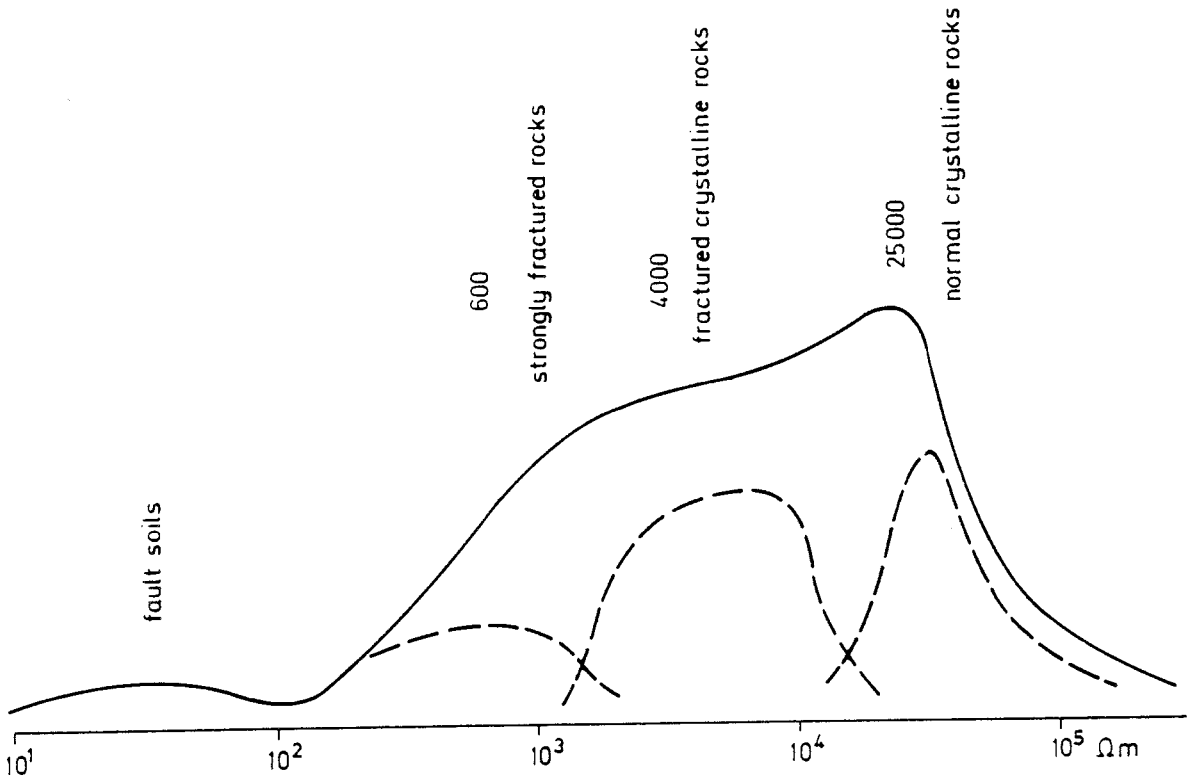

Fig. 5. Second layer (bedrock) resistivities from combined interpretation of ground VLF resistivity and (small coil separation) slingram measurements.

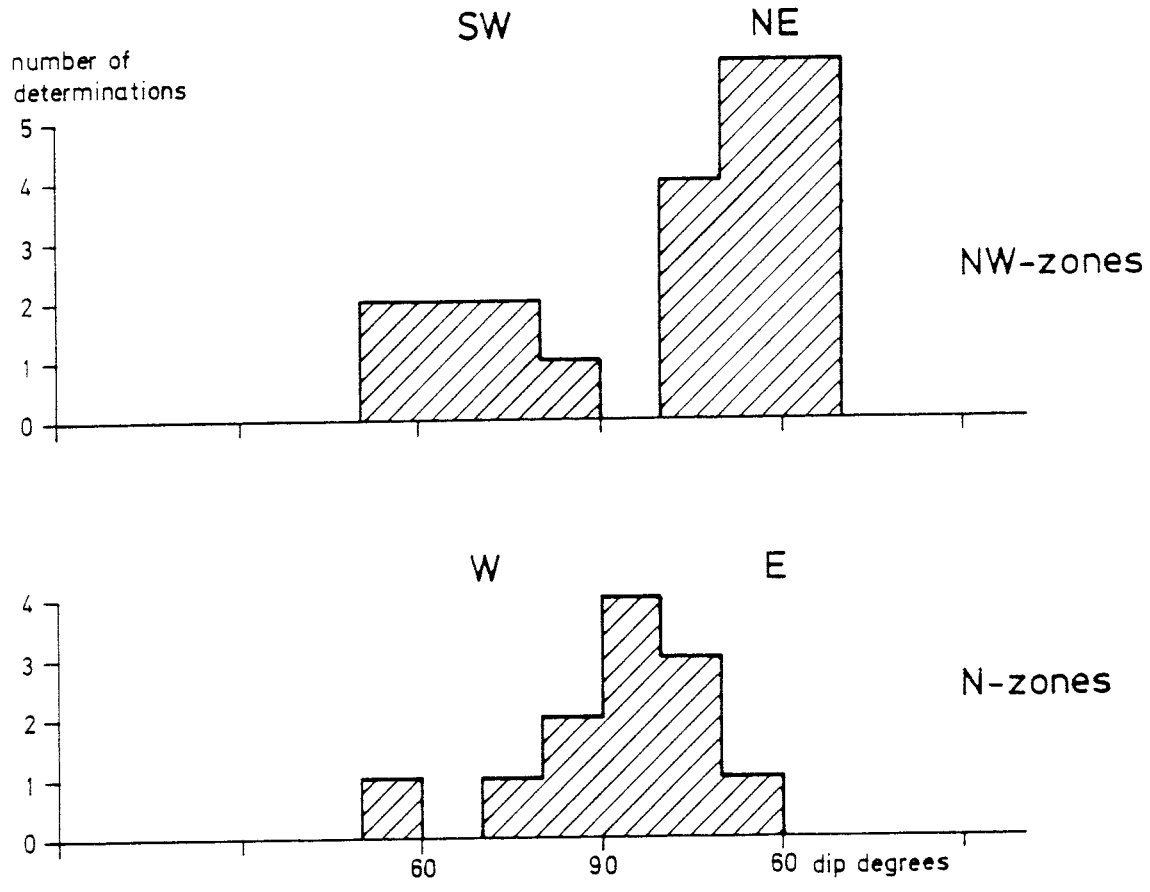

Fig. 6. Dip determinations on major NW and N-trending fault zones.

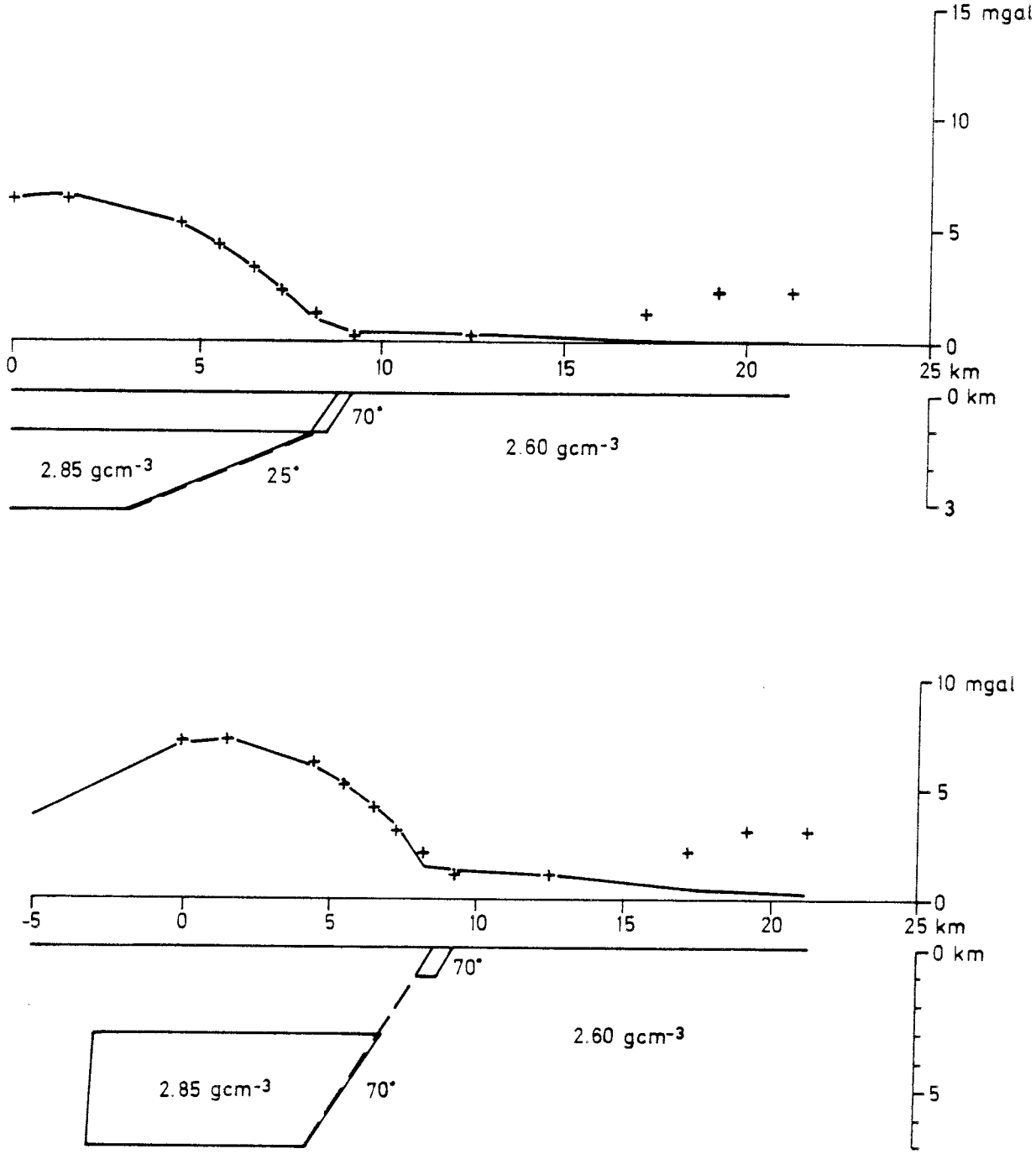

Fig. 7. Combined magnetic and gravity dip determination of NW zone F. (location in map area 26L 5a)

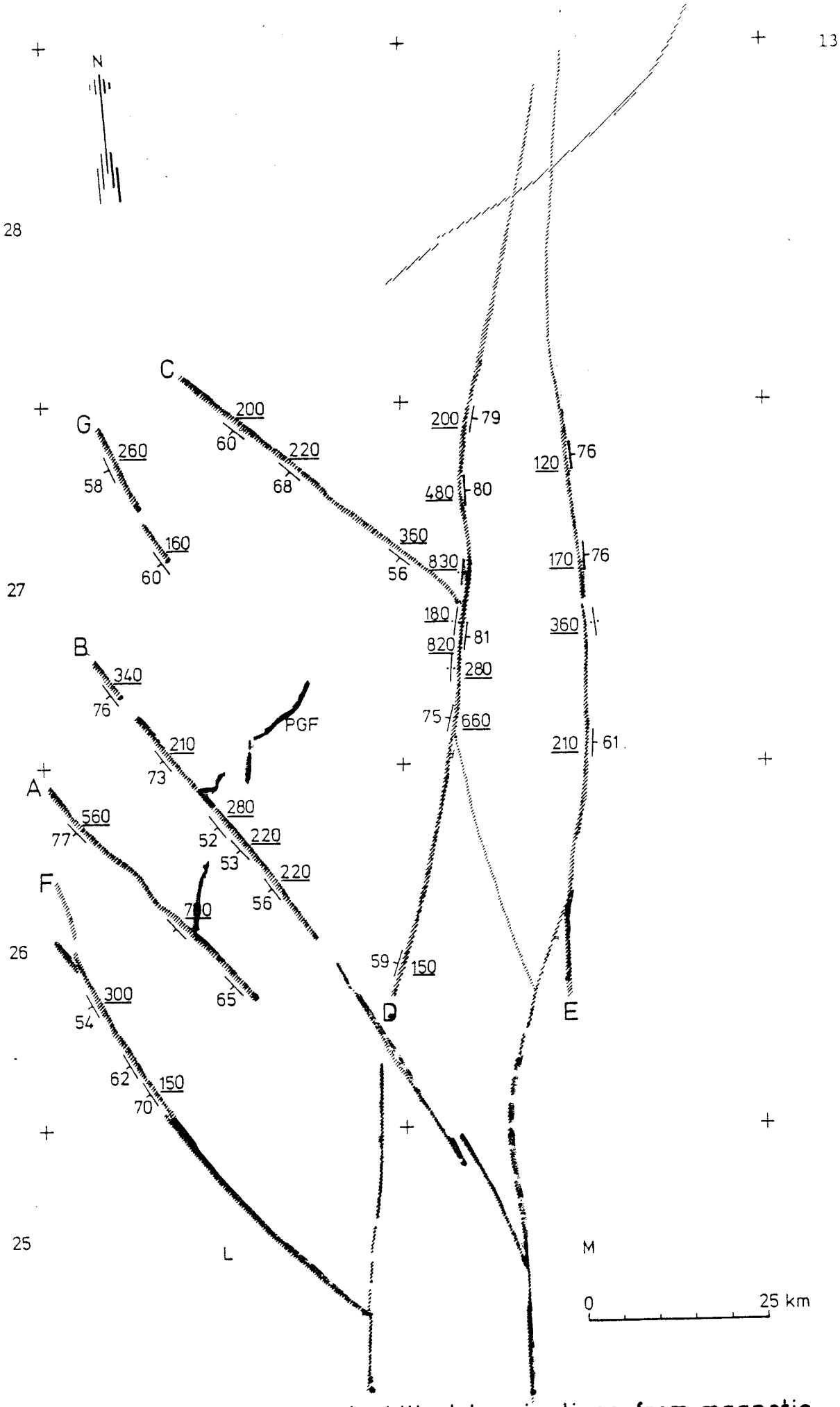

Fig. 8. Results from dip and width determinations from magnetic modelling. Dip in degrees and width in m underlined.

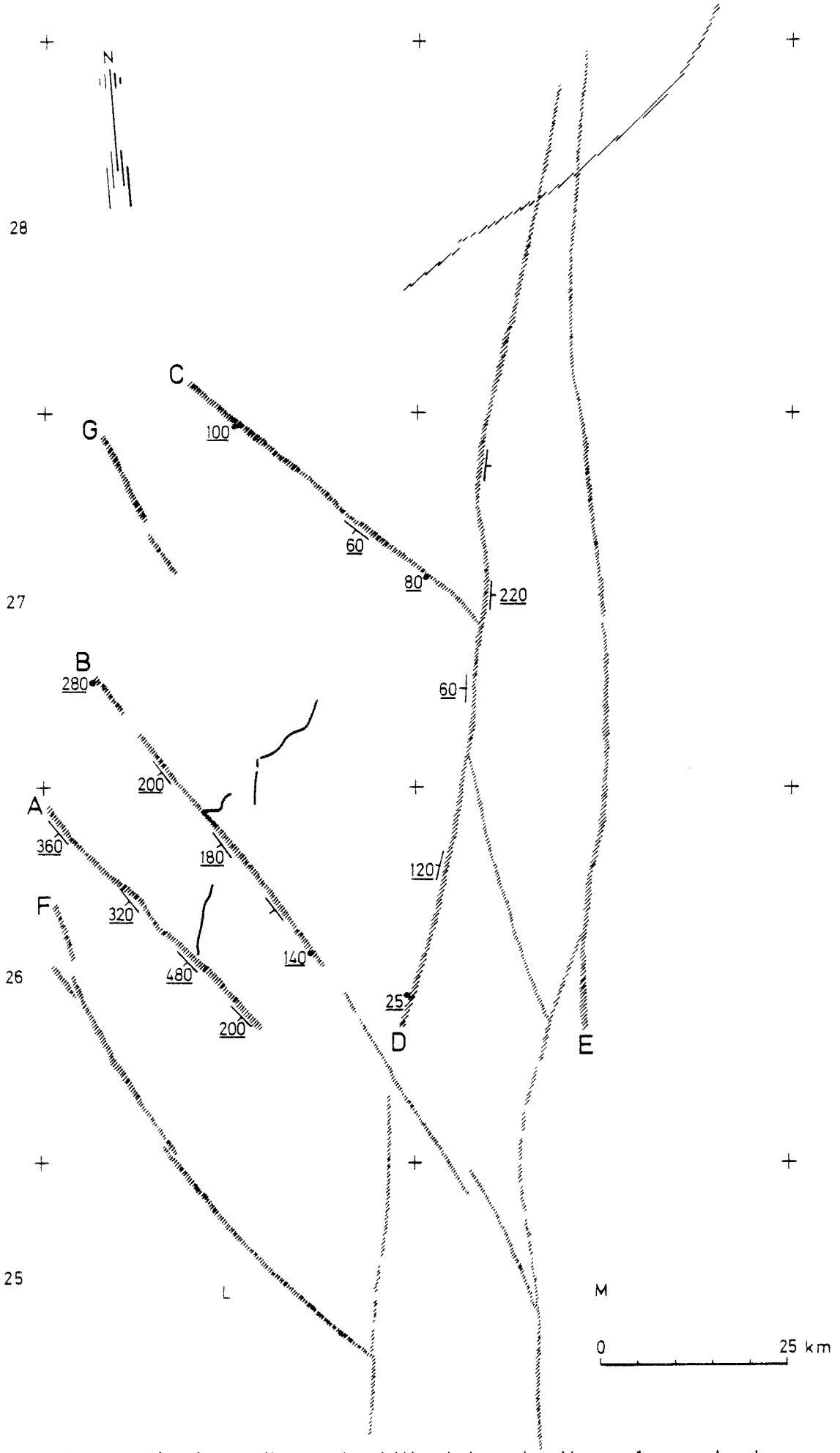

Fig. 9. Results from dip and width determinations from electromagnetic interpretation. Underlined figures denote width in m.

3.2 TECTONIC INTERPRETATION MAP, plate 6

The tectonic interpretation map illustrates the interpretations of the aeromagnetic measurements, the terrain elevation and morphology, and the model calculations. A classification of smaller shear lenses and other morphologic features indicative of positive and negative block movements has also been attempted. Maximum resolution of all the datasets has been used in the digital image analyzing system EBBA II. In this system, the primary data are stored as image matrices 500 x 500 x 255 while interpretations are made and stored in up to 7 graphical matrices 500 x 500 x 1, each with its own color. The following steps were performed in areas 50 x 50 km in size:

- updating of previous aeromagnetic interpretations and digitazation,
- updating using aeromagnetic anomalies and their relief,
- updating using terraine elevation relief,
- classification of shear lenses using updated lineaments and terrain elevation,
- dip determinations, names and other symbols added,
- plot of all graphical matrices to a map in 1:250 000 scale.

Three distinct systems of lineaments dominate the study area, the steep NW-SE and N-S striking zones and the low angle dipping NNE striking zones. In addition, weak E-W and SW-NE striking morphologic lineaments occur. The steep systems contain a number of very prominent fault zones in a lens like pattern. These lenses are more elongated in the N-S system. Each swarm of steep lineaments make up an approximately 50 km wide fracture zone in which the dominant movement has been strike-slip. Significant accumulated displacements of different kinds of Precambrian reference structures can be seen in the aeromagnetic data. Morphologic features appear also to be displaced.The N-S trending system of lineaments is associated with a major break in the gravity anomalies. This indicates very different crustal structures on either sides and very large accumulated block movements. This zone has been called the Baltic-Bothnian Megashear by Berthelsen and Marker (1986), who suggested that it started to be active at about -1.8 Ga. Figures 10 and 11 and the tables in the next sections show the location and patterns of the 3 major fault zones. Together, these 3 fault zones define a 3-dimensional regional pattern.

A set of 14 profiles (A-N in the tectonic interpretation map) have been prepared, in Henkel (1988), which demonstrate various aspects of the magnetic and morphologic structures associated with different fault zone segments.

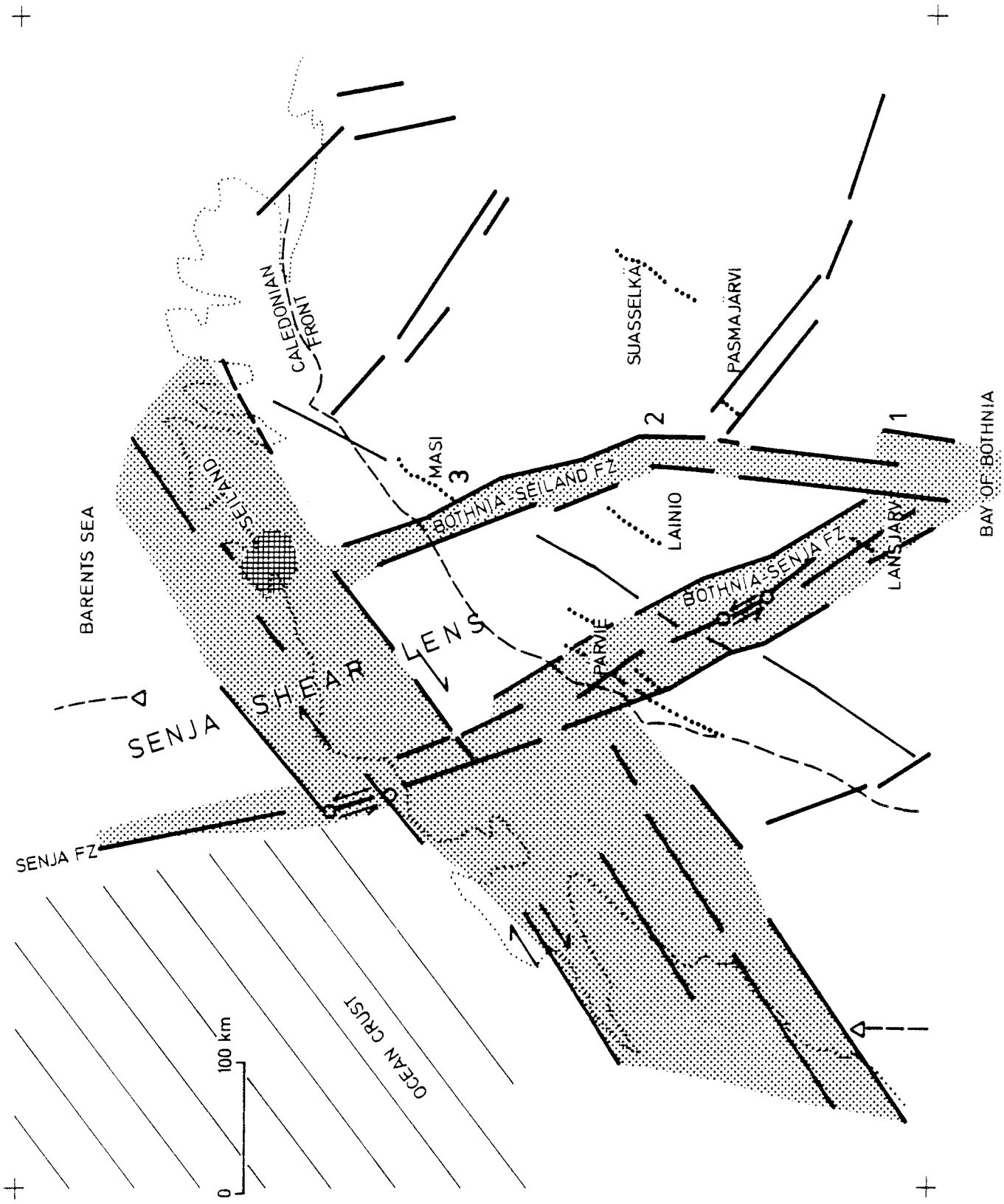

Fig. 10. Generalized regional fault zone patterns in northern Fennoscandia. Dotted lines show known PGF scarps (and their names). 1, 2 and 3 are locations with major lithological discontinuities. ▦ Seiland intrusive province.

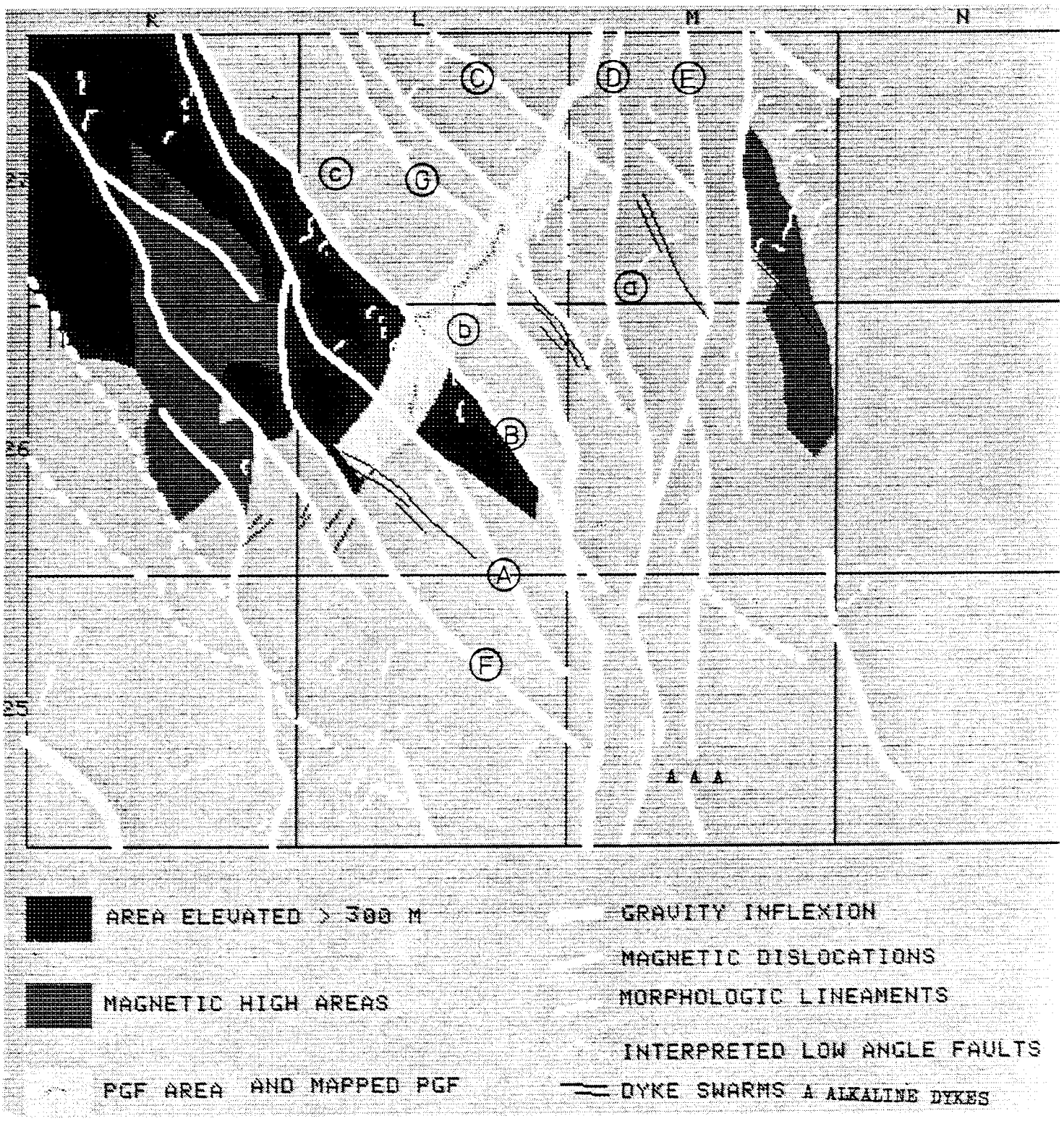

Fig. 11. Compilation of regional lineaments. Each square is 50×50 km. Reference to map system at frame. Letters A-G and a-c denote some of the major fault zone segments treated in the text.

3.3 THE NW STEEP SYSTEM OF LINEAMENTS

In the following table the general properties of this lineament set are summarized. The map of figure 11 shows the main fault zone segments in the study area. Letters A-E refer to the report by Arkko (1987), and fig. 11.

fault zone	lens dimensions (km)	number of fault zone segments	segment nr	length (km)	width (m)	dip (degr)	recent sense of movement
NW trending	95 x 20	5-6	-	>500	75 km		dextral
			A	100	350	70	D
			B	150	200	60	D and S
			C	>50	200	60	D
			F	110	225	60	D
			G	70	200	60	S

This approximately 75 km wide system of up to 5 prominent single faults can be followed NW from just north of the Bay of Bothnia to and beyond the Island of Senja off the Norwegian coast. In several locations very drastic changes in the magnetic patterns are observed indicating large displacements. Contours of the depth to the magnetic basement in the Aeromagnetic Interpretation Map of Northern Fennoscandia (Henkel 1986) show a change in the occurrence of late Proterozoic basin which are more frequent to the SW of the fault zone. It is not yet possible to determine the distribution in time of these displacements. In the Caledonides however, less drastic but clearly visible effects along NW lineaments are found in the region north of Torne Träsk (see map by Gustavsson (1974). The southwesternmost of the NW trending lineaments is indicated by only a sharp morphologic feature - the Lule Älv valley. Displacements in magnetic reference structures are lacking, indicating that only rather small (less than 200 m) block movements can have occurred. Where the lineament bends in the map area 25 K, a large negative shear lens has developed. To the SW of this lineament, the fault pattern changes into an angular block type pattern with only minor block movements. Such angular patterns are typical for the regions between the large shear zones. Locally in the Precambrian terraines, rock foliations are turned into the strike of the NW zones. The general morphology is also strongly influenced along these zones, it therefore appears likely that the NW striking fracture zones have been active since the Precambrian (and may be so at present). One of the larger lineaments acted as a local side wall to the Lansjärv PGF west of b in fig. 11. Other indications of very recent activity can probably be found, such as local fault scarps associated with shear lenses of different attitude. Small negative shear lenses (i.e. pull apart basins) are most likely candidates as indicators of

recent strike slip movements. A number of such features are indicated in the tectonic interpretation map and should be field-checked. The general trend of the Lansjärv PGF is between 3 major NW lineaments. The PGF however, terminates within the shear lenses associated with these lineaments, indicating that such lenses act as strain traps and were deforming simultaneously (fig. 12). In Henkel and Wållberg (1987), an analysis of these features is made, based on detailed ground geophysical measurements.

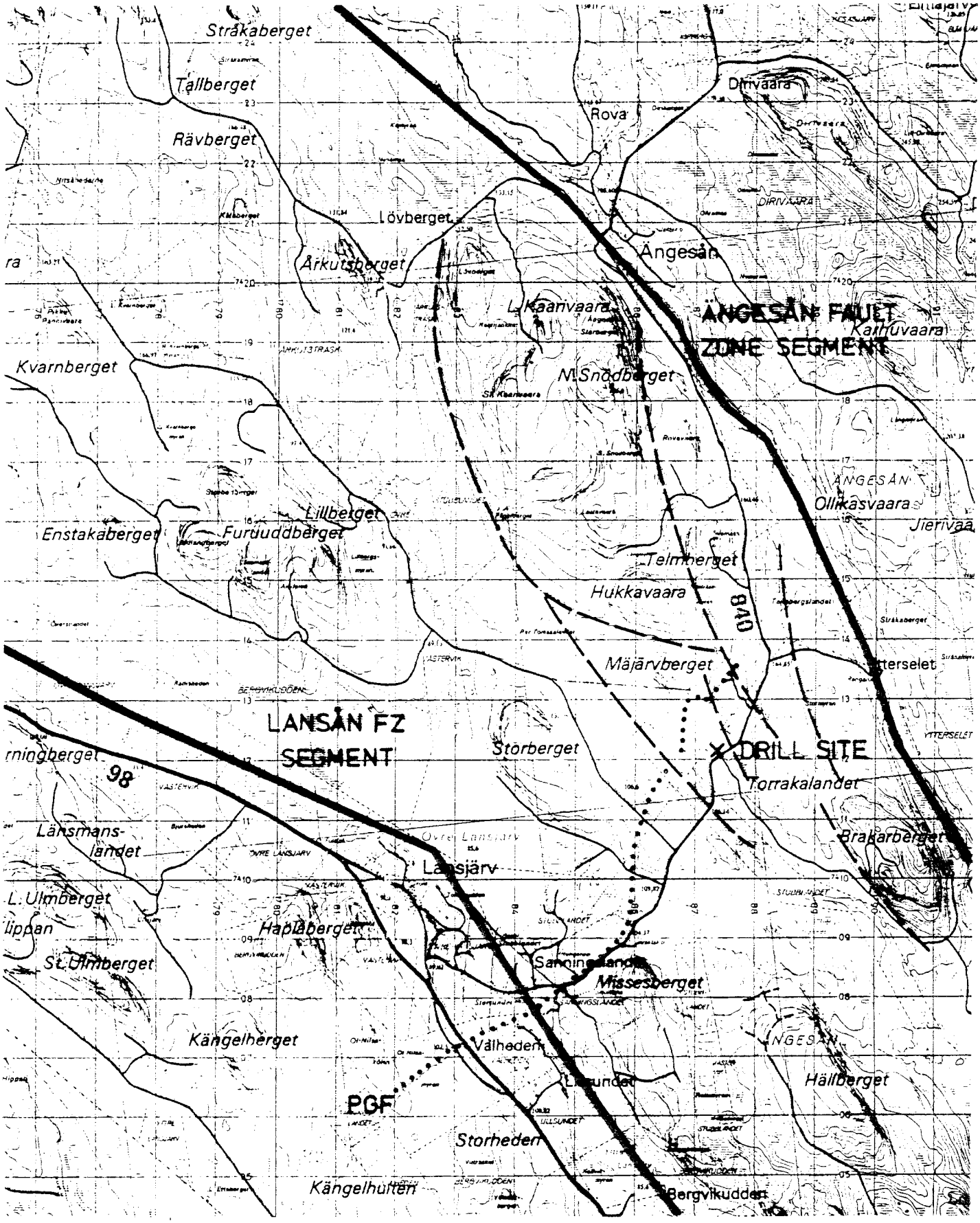

Fig. 12. The northern termination of the Lansjärv PGF in the Telmberget positive shear lens (10×4 km). Map area 27L 3g. Each square is 1×1 km.

The dip of NW striking major fracture zones is on average 60 degrees to the SW. Figure 6. Edges of some associated shear lenses dip in the opposite direction, i.e. 60 degrees to the NE. These dip determinations are based on model calculations of ground or aeromagnetic profiles located at characteristic parts of the lineaments. The magnetic model calculations can not resolve the zones deeper than about 5 x their width (i.e. about 1 km depth), although the zones may continue to larger depths. The structural pattern arising from the present knowledge is that of a 3-dimensional network of shear zones of different magnitude, dipping to the SW in its top 1 km. The combined use of magnetic and gravity modelling may however give a clue to the deeper structure of this network. The following two hypotheses can be considered, fig. 13.

a - the present erosion level is a random surface through a 3-dimensional network of shear zones with similar horizontal and vertical geometry,

b - the observed 3-dimensional network is the result of the proximity to a free surface which can deform vertically. The network changes geometry deeper in the lithosphere.

In the case a, the deeper structures of the fracture zones would be similar to the horizontal sample we look at, down through the brittle part of the crust where it would change to a ductile set of structures continuing down through the lithosphere - this is illustrated in figure 13. This hypothesis also requires a continuous variation in the dip of single fracture zones from SW over vertical to NE - the vertical dips being the most frequent (as the lenses are elongated in plane). This configuration is rather similar to that presented in Sibson (1977).

In case b, a structural anisotropy is caused by the steadily upward decreasing vertical load and the occurrence of a discontinuity at the surface. Shear lenses would only develop in the uppermost regions of the brittle crust. The larger shear zones would have a continuous dip down and through the ductile regime of the crust.

Case c is like b, but the fault zone narrows in the ductile regime of the lithosphere due to strain concentration. This effect may however depend on the rate of displacements, being pronounced in periods of strong motions only. The strain concentration is obtained by thermal softening due to frictional heating (Brun and Cobbold 1980).

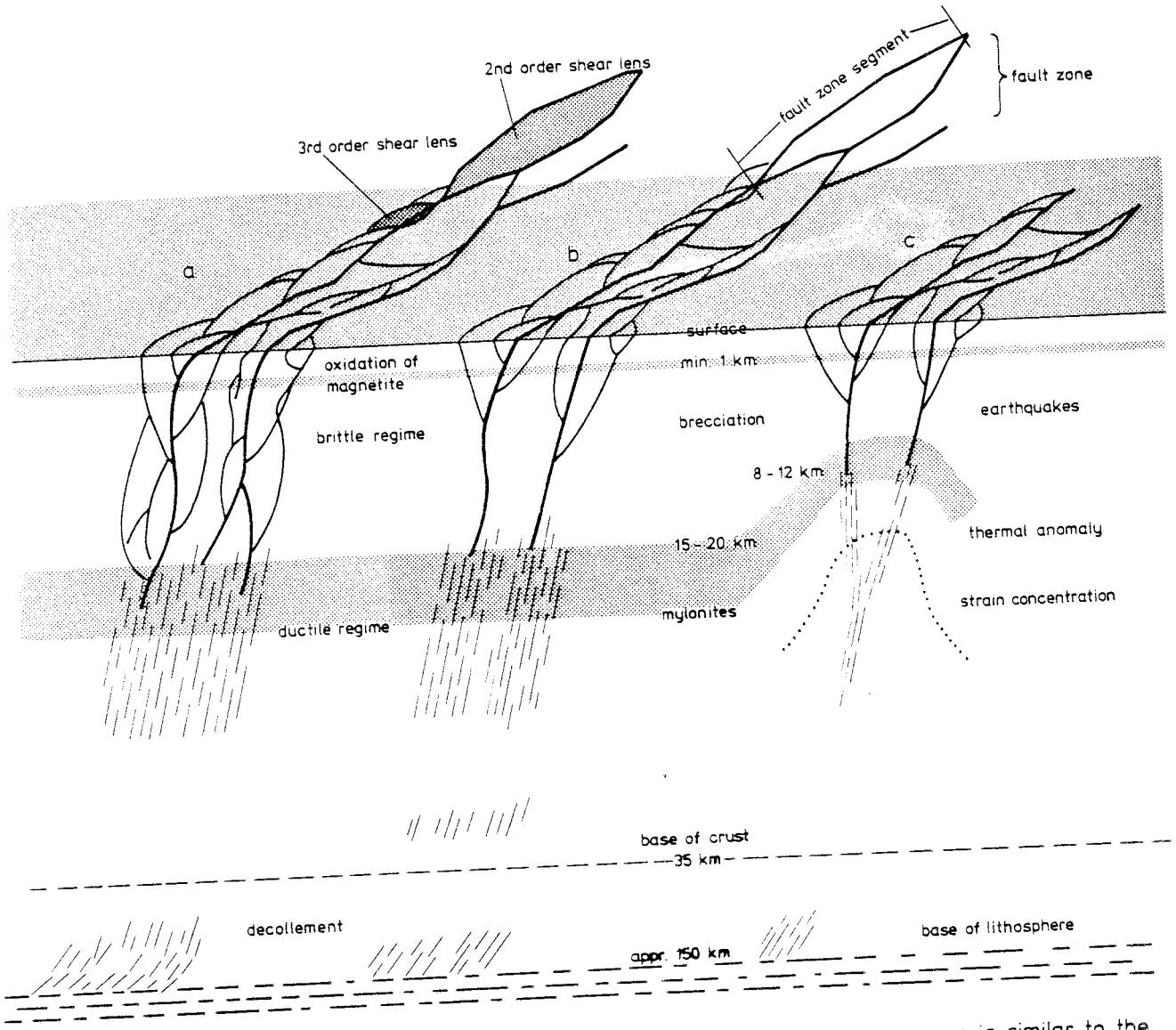

Fig. 13. Deep continental faults. Model a with downward continuing network of shear zones is similar to the model of Sibson (1977). In Model b the fine structure of the network increases towards the free surface. Model c is similar to b but with higher strain rates leading to thermal softening at depth (and rise of the brittle-ductile transition). See also Brun and Cobbold (1980).

3.4 THE N STEEP SYSTEM OF LINEAMENTS

In the following table, the general properties of this set of lineaments are summarized. The map of figure 11 shows the main fault zone segments in the study area. Letters D-E refer to the report by Arkko (1987).

fault zone	lens dimensions (km)	number of fault zone segments	segment nr	length (km)	width (m)	dip (degr.)	recent sense of movement
N trending	105 x 10	3-4	-	650	45 km	steep E	sinistral
			D	120	200	80	S
			E	120	200	75	S

This approximately 45 km wide system of faults and lineaments can be followed from the Bay of Bothnia to the Seiland mafic intrusive province in northern Norway. In the study area, 3-4 distinct and prominent single zones are noticed. The magnetic patterns are entirely different on each side of the fault zone. On the entire length of the zone, 3 very prominent angular discontinuities are seen in the magnetic patterns (for location, see fig. 10).

1 - in the southern area 25-26 N, the distinct east-west banded pattern occurring east of the fault zone terminated and does not re-occur within the study area,

2 - in the central area at Pajala-Kolari (to the north of the study area), a possible large sinistral shift of magnetic patterns associated with an early Proterozoic greenstone belt can be seen,

3 - in the northernmost area, a strong angular discontinuity occurs between SW striking early Proterozoic greenstone structures of the northeastern block and NNW striking greenstones of the SW block.

As the main gravity inflexion lies to the west of the westernmost N-trending fault zone, a general W dip can be inferred in the upper 10 km of the crust for this fault system.

Over large areas, the rock foliation turns into the north-striking fault system (see geological map area 25M). The gravity anomalies reflect large scale density contrasts and changes in crustal composition and thickness. Low gravity in the eastern block changes to high gravity in the western block along a pronounced gradient close to the westernmost major magnetic lineament. Model calculations of these gradients indicate a major step of about 5 km down to the east in the crust of intermediate composition (Arkko 1986). In this respect the north-striking system of faults represents larger accumulated displacements than the NW-system. It is yet not possible to determine the sense and

amount of displacement along the N-S-system but it appears to be very large sinistral. Magnetic model calculations show steeper dips, on average about 90 degrees (with both east and west local deviations). The general appearance of single major zones is similar to the NW system. Associated shear lenses are numerous and several show possible post-glacial deformation. An example is shown in fig. 26. The shear lenses associated with the N-system appear also to be more elongated than those in the NW-system of faults. Some of these shear lenses contain highly magnetic granites which may be of deep origin. Several disconnected NW-lineaments occur in between major northtrending fault zones and some of these also show indications of recent movements. These lineaments strike more to the southeast, indicating a dextral rotation of the blocks between the single north-striking lineaments. An alternative explanation would be significant block movements which have emplaced blocks with a different interior fabrics. The N-S-lineaments continue southwards into the Bay of Bothnia. One defines a distinct step in the bottom morphology just south of the study area associated with the occurrence of Jotnian and Cambrian sediments in the eastern block (Ahlberg 1986).

3.5 THE NNE NEAR HORIZONTAL SYSTEM OF LINEAMENTS

In the following table, the general properties of this set of lineaments are summarized. The map of figure 11 shows the main fault zone segment in the study area. Letters a-b refer to this report.

fault zone	lens dimensions (km)	number of fault zone segments	segment nr	length (km)	width (m)	dip (degr)	recent sense of movement
NNE trending	50 x 2.5	3-5	-	>50?	8 km	gentle SE	?
			a	35	<300	<5	
			b	90	<500	"	
			c	50	<300	"	

These lineaments constitute sets of topographic scarps, most of which have steep WNW facing slopes. The foot of such slopes is thought to represent zones of weakness allowing erosion to remove the zone proper and to cut down to the more resistent parts below and thus forming a gently dipping flat area to the NW of the scarps. The slope of such gentle ESE dipping zones is determined by the stratum contours of the fault scarp as it turns around hills. It is generally low and only 1-5 degrees to the southeast. Geological field control Talbot (1987) and VLF profiles show associated flat lying foliations and asymmetric anomalies typical for gently dipping conductors. (Figure 14C.) Asymmetric magnetic lows

are locally associated with these fault zones. The most obvious of the PGF movements appear to have occurred in zones parallel to these lineaments. Figure 14C shows the distribution of dip estimation of these zones.

In figure 11, all so far determined gently dipping lineaments are shown with thin white lines. In all 5 sets of such zones appear, each 5-10 km wide, at the surface (representing a width of approximately 300 m) and with 30-40 km spacing between zones in the horizontal (representing a spacing of approximately 2.5 km). The gently dipping zones are interrupted by the NW and N striking fault systems indicating simultaneous movements of all 3 systems or younger movements of the steep faults.

Some other characteristic morphologic patterns seem to be associated with the gently dipping zones. Rather steep hillsides above several of the indicated zones rise, to form a WNW oriented wedge. Gentler dips are observed to the east. Within these wedges numerous gently dipping surfaces appear, so that the wedge resembles a pile of thrust flakes. These structures rise above the average elevation of the surroundings.

Apart from the 3 major fault systems, no other dislocation directions seem to occur on the regional scale. In a few places, especially in the southwestern area, minor east striking lineaments can be observed in the morphology and the relief of the elevation data. These and other similar structures with small extent (and normally not visible in the aeromagnetic data) are indicated with a separate color in the map. Some represent rather sharp structures and may be of recent origin. Smaller features, clearly discordant to the glacial structures, may be of post-glacial origin and are indicated as suspected PGF:s.

Figure 14C

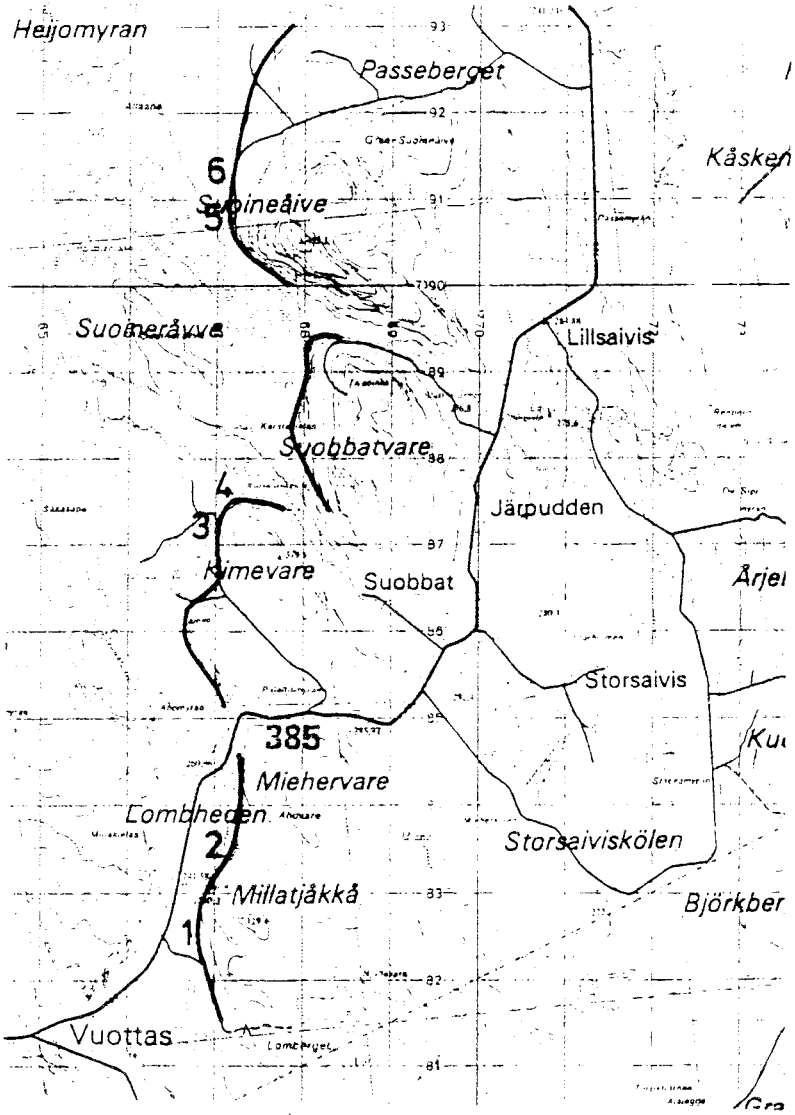

Location of VLF test measurements across gentle SE dipping fault zone.

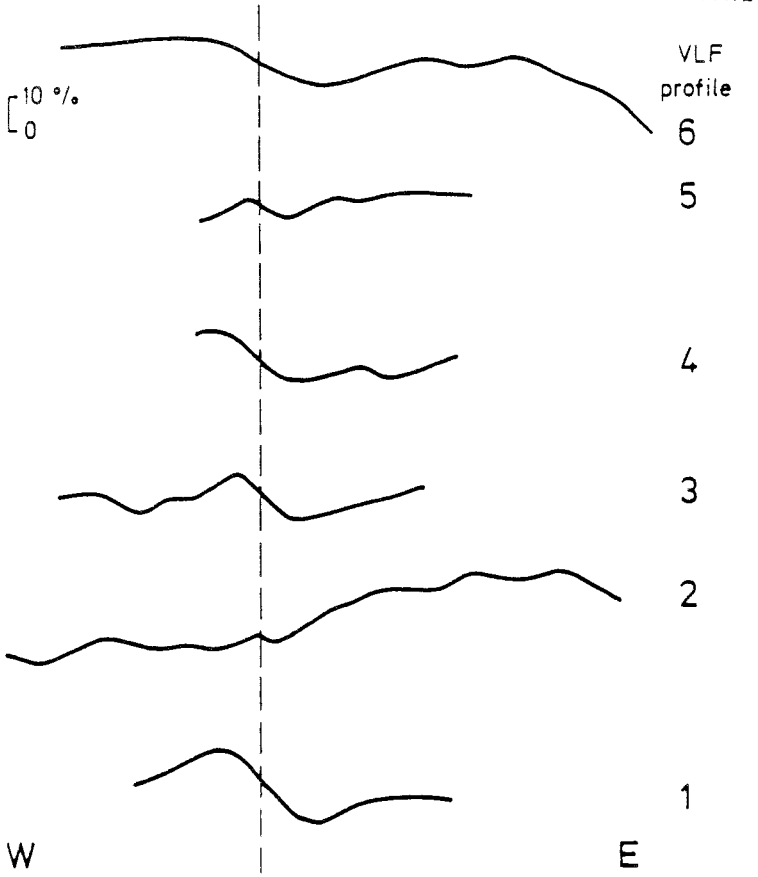

VLF test profiles

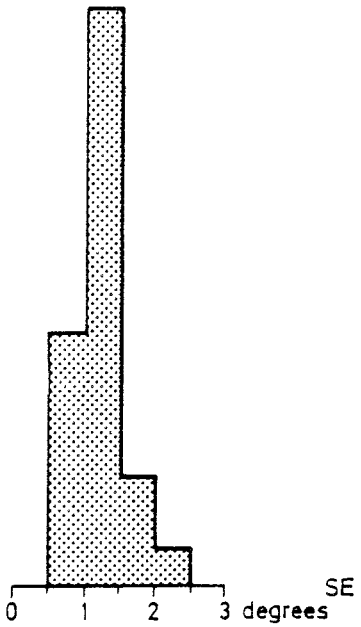

Distribution of dips of all gently SE dipping zones.

3.6 HIGHEST SHORE LINE (HS) DETERMINATIONS

The map of the location of the highest (post glacial) shore line is constructed from stereoscopic elevation determinations on a large number of sites of different type. All determinations are reported in Sundh and Wahlroos (1987). These data were compiled to a separate 1:250 000 map. The average accuracy is about 3 m.

The HS pattern shows a general curving trend around the Bay of Bothnia. The minimum elevation is around 160 m and the maximum elevation is around 220 m. Only a few meters local changes can be seen and it is uncertain if these reflect differential block movements. Therefore the regional trend of the highest shoreline has been constructed by smoothing the 10 m contours and by interpolating intermediate 1 m contours by eye. This smoothed bend is shown in fig. 14A. Next the differences between observed elevations and the regional trend were calculated. Numerous areas with deviations from 0 occur. The map area can be divided into three regions with different aspects of the HS deviations from the regional trend. This division follows the westernmost N-trending fault zone and the southwesternmost NW-trending fault zone. In fig. 14B a comparison is made between the distribution of the HS residuals in each area. Area II, which lies in the central part of the study area (where the regional trend is best defined), shows a positive residual distribution which is centered around +2.2 m (above the regional trend). Area III shows a negative distribution around -2 m (below the regional trend) and area I shows both a small negative and a positive residual distribution. The distributions around 0 deviation indicate the scatter in the observed HS values and in the regional fit.

The results can be interpreted as a slight rise of the central block of about 2 m with respect to surrounding areas and a slight subsidence of block III of about 2 m. The local distribution of residuals, together with the location of major fault zones, may indicate areas where measurable displacements of HS occur. More precise levellings of the indications would improve the resolution of this method in those particular areas. The expected displacements due to tectonic disturbancies during the last 8000 years are rather small but the obtained results encourage further studies.

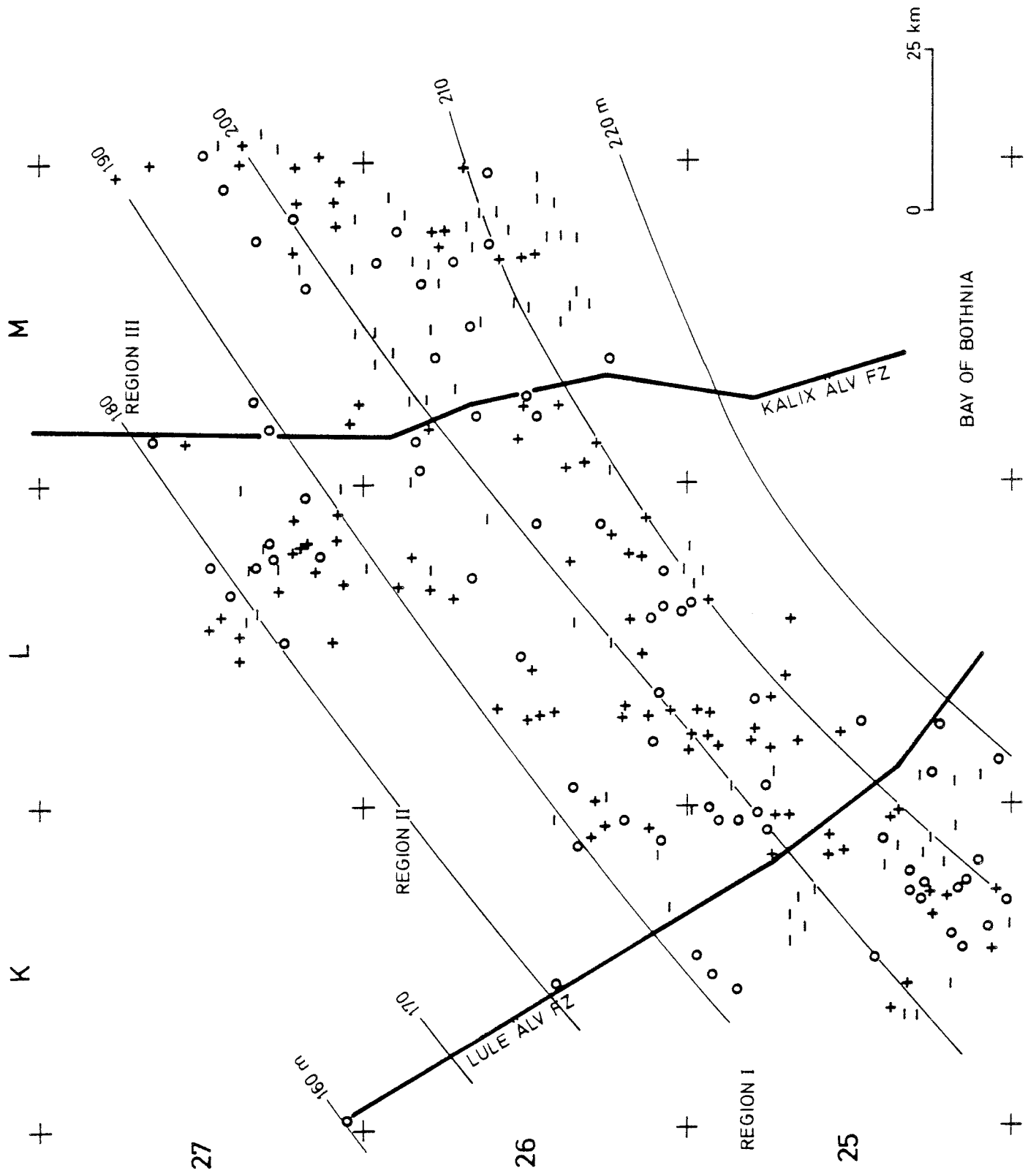

Fig. 14A. Distribution of HS determinations and regional trend. + - o show locations with positive, negative and no deviation from the regional trend, respectively.

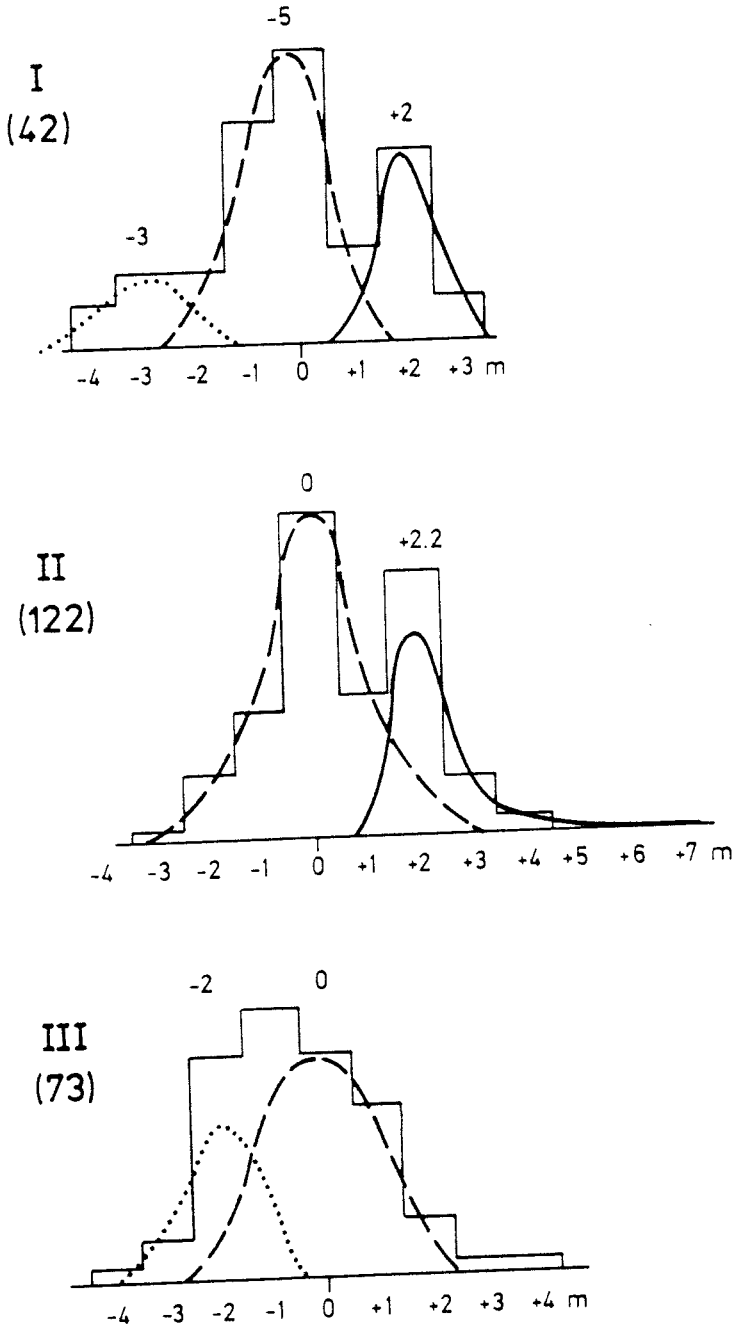

Fig. 14B. Deviations (in m) from regional HS trend shown in fig. 14A for three regions I-III. The number of HS observations is given in brackets. Map area 25-27 K-M.

3.7 THE POST-GLACIAL FAULT SCARPS, PGF

The post glacial fault scarps have previously been described in Lagerbäck and Witschard (1983) and Henkel et al. (1983). All geophysical measurements in an inner 40 x 20 km area around the faults are documented in Henkel and Wållberg (1988). The previous known faults consist of a northern, almost 15 km long scarp facing towards NW, with different scarp heights, an approximately 10 km long irregular scarp facing NW, having its sidewall in a prominent NW oriented fault zone segment, an appr. 5 km N-S oriented scarp facing east in the central area and a southern, about 5 km long scarp facing WNW. Figure 15. All branches except the Central N-S striking one appear to dip gently to the southeast or east. As there is normally rather small topographic relief, the dips can be estimated with stratum contours only at Mäjärvberget, where it is about 12 degrees and at Storsaiviskölen, where it is about 10 degrees. The seismic refraction profiles of these low angle branches are shown in figure 16 (left side from north to south). In these profiles, the topographic scarp is usually located above a bedrock surface inclined in the opposite direction. In some profiles, this surface rises again to the southeast or east. In profile 26 at the souther branch, the bedrock surface rises under the scarp. Contrary to these configurations, the bedrock surface rises under the elevated terrain in the N-S oriented fault scarp and in the sidewall of the Risträskkölen thrust flake. These faults therefore, have been interpreted as steeply dipping. Figure 16, right side. The postglacial faults appear to interact with NW-trending major fault zone segments and with minor NW-trending faults (indicated in figure 15, Henkel and Wållberg op.cit.). At the northern and southern terminations, the fault scarps disappear in the 3rd order shear lenses associated with large NW-trending fault zone segments.

Terrain relied studies in the area reveal several rather sharp minor steps in the terrain which can be interpreted as fault traces. These indications are shown in figure 17. The nature of these structures should be field checked. The entire set of PGF scarps is located within an approximately 5 km wide zone with several gently dipping faults interpreted from topographic maps and elevation data. This zone is about 60 km long and appears to be interrupted by transecting NW fault zone segments. The location of the PGF scarps within this NNE-trending zone indicates that most of the post glacial fault movements may have occurred by reactivation of faults of the NNE trending gently dipping fault zone.

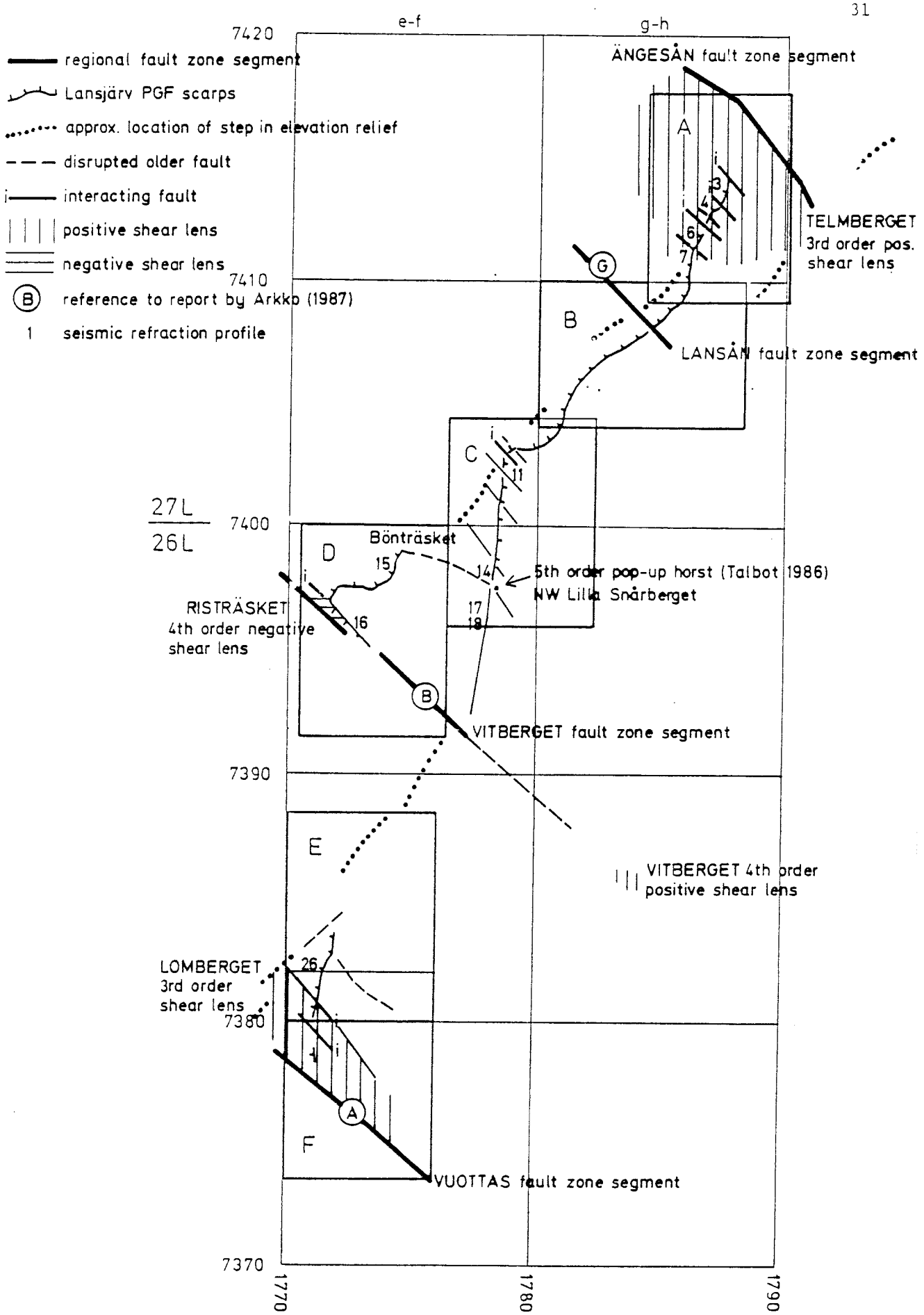
regional fault zone segment
Lansjärv PGF scarps
approx. location of step in elevation relief
disrupted older fault
interacting fault
positive shear lens
negative shear lens
reference to report by Arkko (1987)
seismic refraction profile
e-f
g-h
7420
7410
7400
7390
7380
7370
1770
1780
1790
27L
26L
ÄNGESÅN fault zone segment
TELMBERGET
3rd order pos.
shear lens
LANSÅN fault zone segment
Bönträsket
5th order pop-up horst (Talbot 1986)
NW Lilla Snårberget
RISTRÄSKET
4th order negative
shear lens
VITBERGET fault zone segment
VITBERGET 4th order
positive shear lens
LOMBERGET
3rd order
shear lens
VUOTTAS fault zone segment
A
B
C
D
E
F
G

Fig. 15

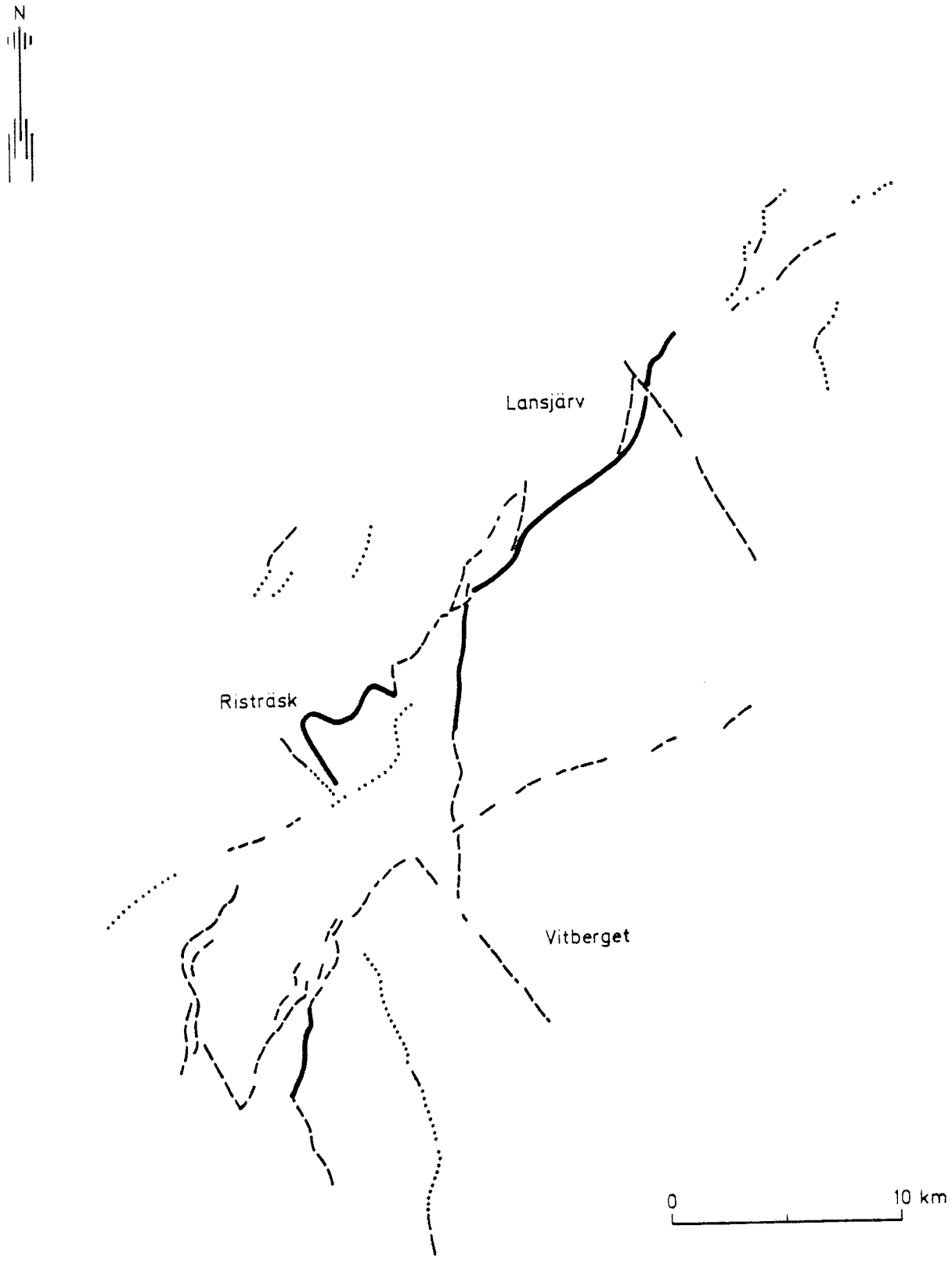

Fig. 17. Interpretation of terrain relief (100 × 100 m) data. PGF scarps and possible late or postglacial fault scarps.

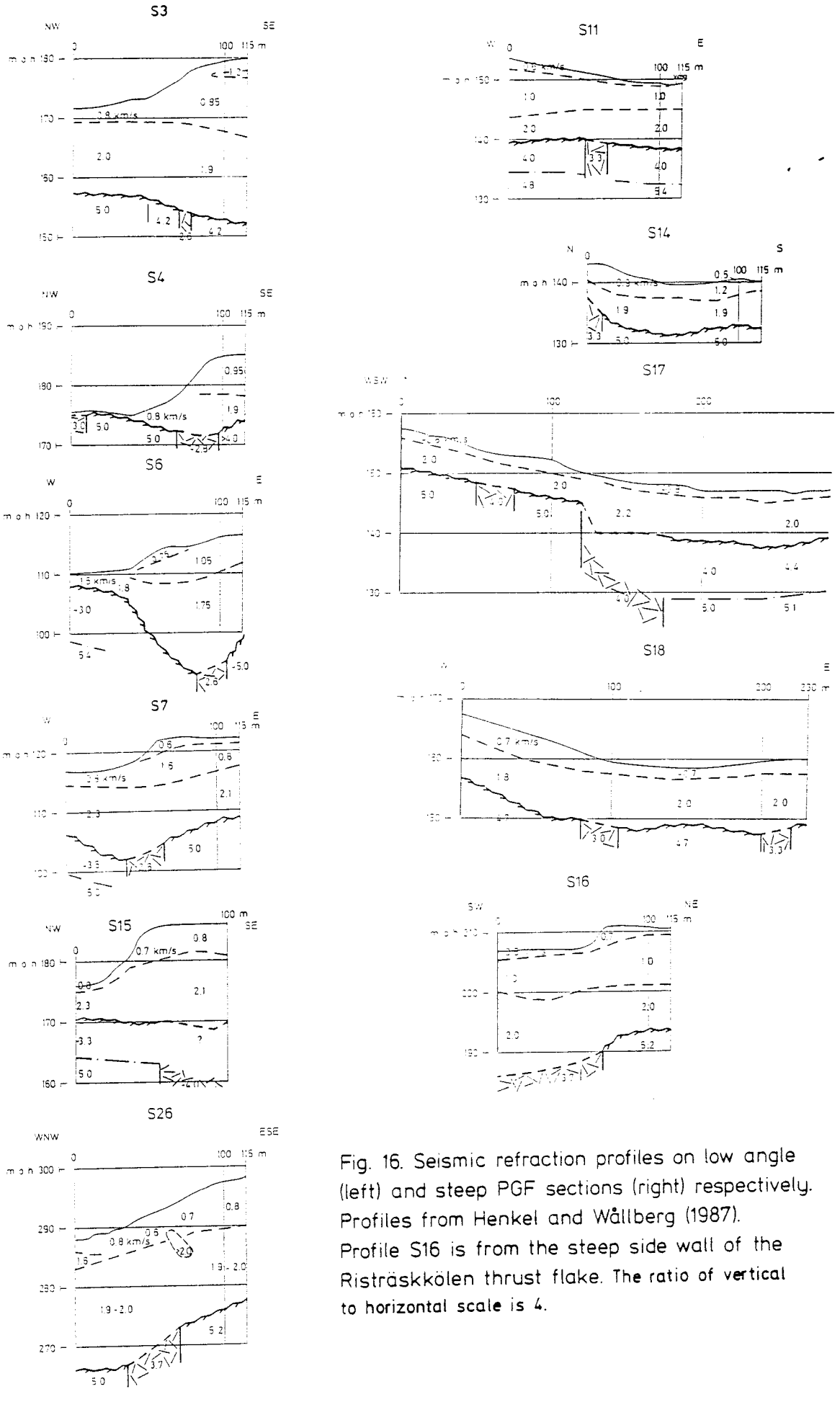

Fig. 16. Seismic refraction profiles on low angle (left) and steep PGF sections (right) respectively. Profiles from Henkel and Wållberg (1987). Profile S16 is from the steep side wall of the Risträskkölen thrust flake. The ratio of vertical to horizontal scale is 4.

4 STRIKE SLIP FAULT PATTERNS

4.1 GENERAL PATTERNS

In the plate tectonic concept, strike slip faults are necessary to accommodate stress from divergent plate motions. Several large strike-slip fault systems have been described in the literature such as the Alpine Fault (In New Zealand), the San Andreas Fault system (in California). Apart from large accumulated ofsets of structures, a typical network pattern of lens shaped structures occurs in the relief. Subsidence basins and horsts with km scaled vertical displacements occur, features which are more obvious than the main fault scarps. As soon as compression or tension is involved in the kinematics, major adjustments of the earths free surface occur. It appears also as if strike slip alone is the least frequent situation. Distribution of earthquakes along a section of the San Andreas FZ occur in an irregular pattern both in strike and perpendicular to the strike as shown in figure 18. All earthquakes are located in the upper 12 km of the crust, thus defining its brittle layer. Aftershocks, following a major slip on the main fault, seem to distribute within adjacent strike slip shear, lenses thereby adjusting the free surface (Sibson 1986). The size of shear lenses varies in scale from crustal to local. The reason for their existence is the tendency to create or destroy space in crust as a response to extension or compression. The associated features at the earth surface include all kinds of faults and folding. Older structures respond to new stress fields by reactivation of suitable fractures. The accumulated effects may therefore be of considerable complexity.

Morphologic studies will however focus on the most recent development of a fault zone. Continued block movements along a fault, will enhance or destroyed earlier structures. Enhancement increases the scale of features while destruction will create a complex pattern of structures. The inversion of earlier features will face the interpreter with especial difficulties. In figure 19, sets of typical strike-slip related features are noted and some might be found in the morphology if sought. See also examples in Deng et al. (1986).

Extensive flow of water can be expected within each fault zone, and a continuous break down into clay minerals will take place down to considerable depth (which varies with the geothermal gradient). Such flows could dissolve and precipitate metals and contribute to the low electrical resistivity observed in fault zones and to the pervasive oxidation (especially of magnetite to hematite), creating typical low magnetic anomalies, Henkel and Guzmán (1977).

The 3-dimensional pattern of strike slip faults is still not well defined. The complex pattern displayed by exhumed fault zones indicated that they penetrate deep into the crust down to highest grade metamorphic conditions. All kinds of fault related structures can commonly be found simultaneously in one zone. These include mylonites, earthquake melts and fault gauges. The faults were thus active when deep. Will the

dips be constant or will the increased lithostatic pressure impose a different structural style? In addition, the lithosphere is laminated, with regard to the distribution of brittle-ductile behavior.

Studies in mines to about 1 km depth indicate a slightly curved shape of fault surfaces, similar to that in the horizontal plane (Wallace and Morris 1979). Figure 20. Magnetic model calculations on oxidized zones in the Lansjärv area, fig. 4, suggest that the surface dip is maintained to about 1 km depth. Gravity modelling indicates a maintained surface dip to about 7 km depth, but at greater depth, shallower dips are also possible. Compressional and tensional stresses may also favor different structural styles as well as the orientation of these stress fields in relation to the fault pattern.

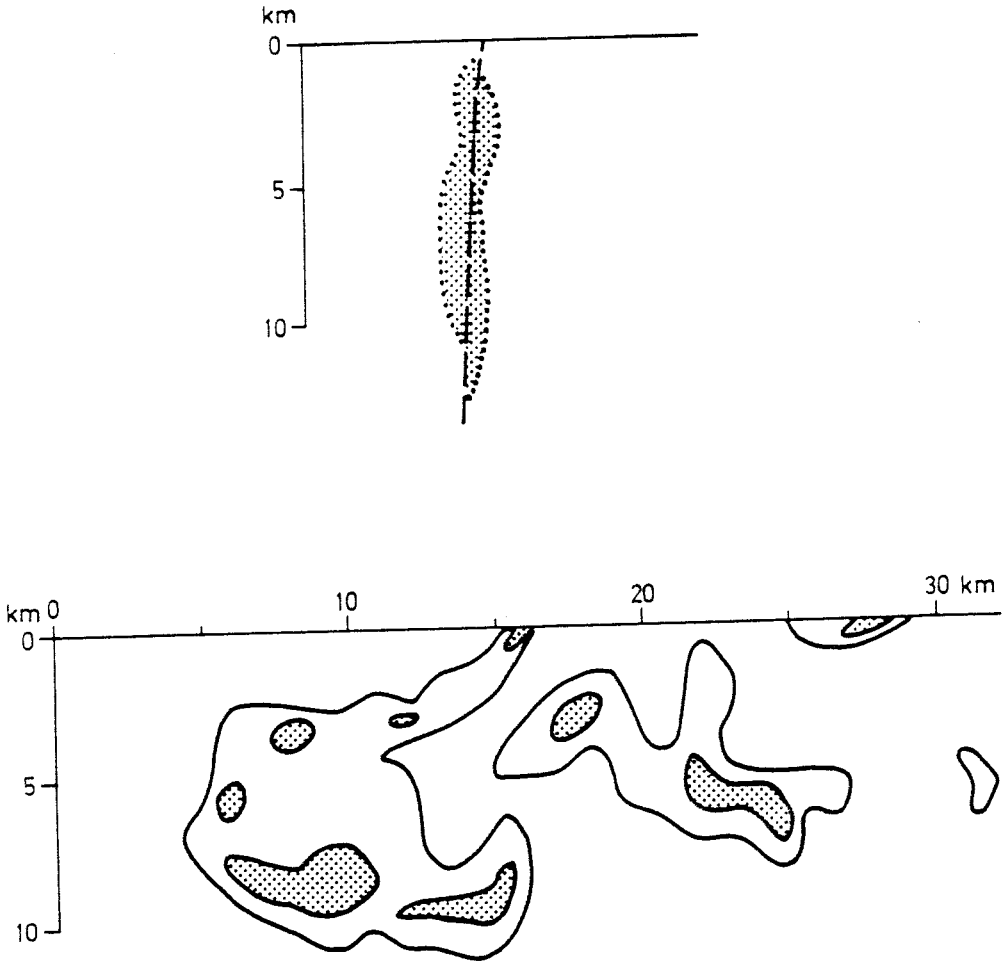

Fig. 18. Distribution of earthquake locations at San Andreas FZ projected in a plane perpendicular to fault strike (above) After Hanks (1979) and parallel to fault strike (below); contours represent 5 and 10 earthquake per unit area during the observation period. After Liechti and Zoback (1979).

SHEAR LENSES
at fault stepover

+POSITIVE
compressional

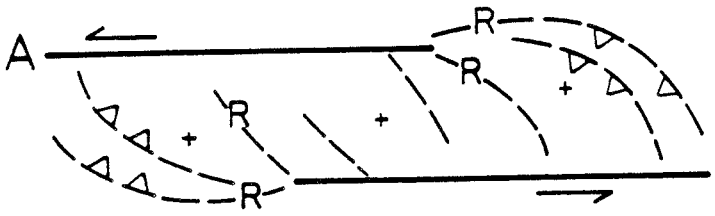

outer thrusts extending beyond major faults, inner reversed faults (R), internal folding

-NEGATIVE
tensional

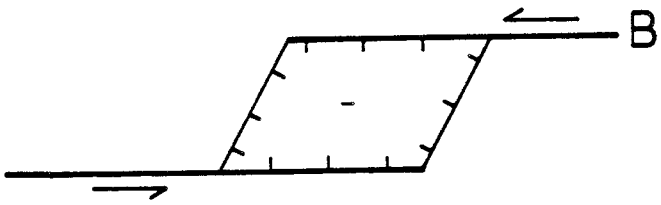

normal faults between major faults one or several subsidence centres, tilting + internal brecciation + hydrothermal activity

PUSH UP HORSTS

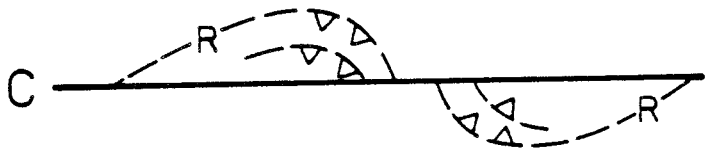

displaced hills as fault cuts through central breccia lens and elevated terrain

PULL APART BASINS

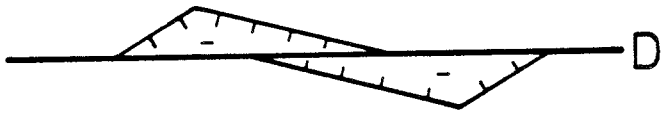

displaced angular lows as fault cuts through breccia graben long lens valleys

E
CRUSTAL SHORTENING THRUST BELTS

F
CRUSTAL THINNING OCEANS

Fig. 19A

at fault bend

+POSITIVE
compressional

-NEGATIVE
tensional

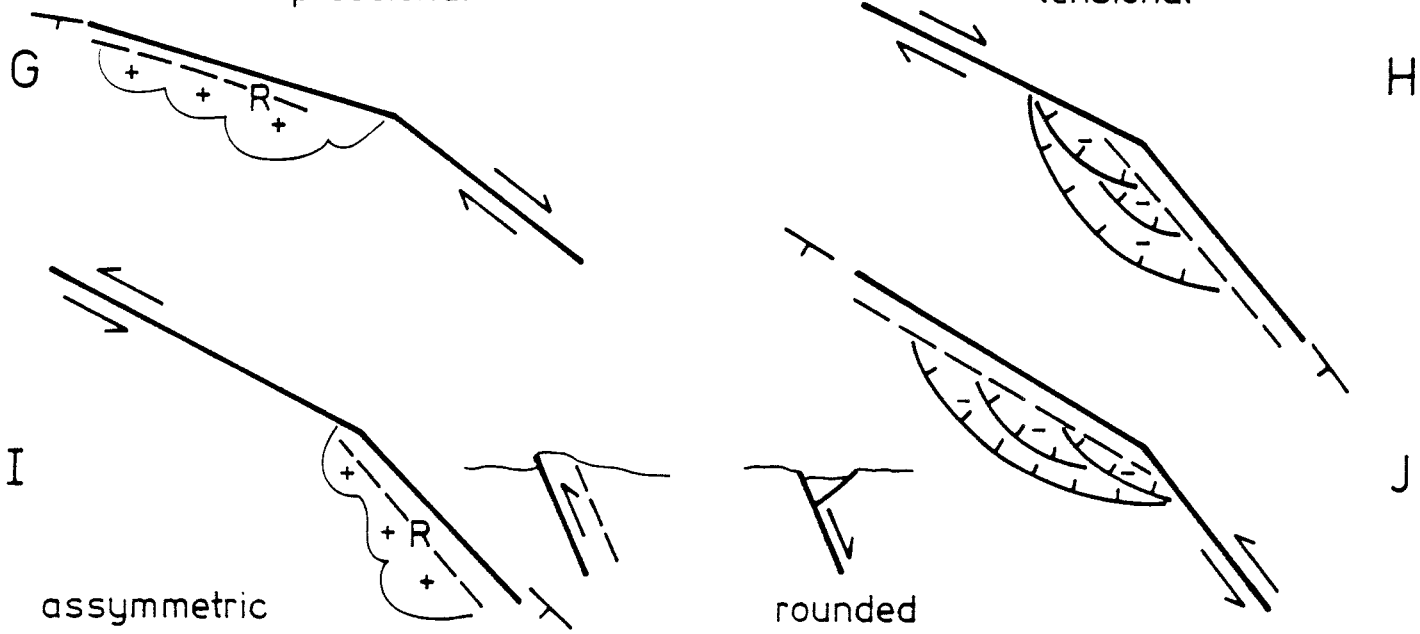

assymmetric compressional horsts on hanging wall

rounded collapse basins cutting outside main fault on hanging wall

DEFORMATION ON REVERSED MOVEMENT

central oblique graben

fault cuts through breccia graben

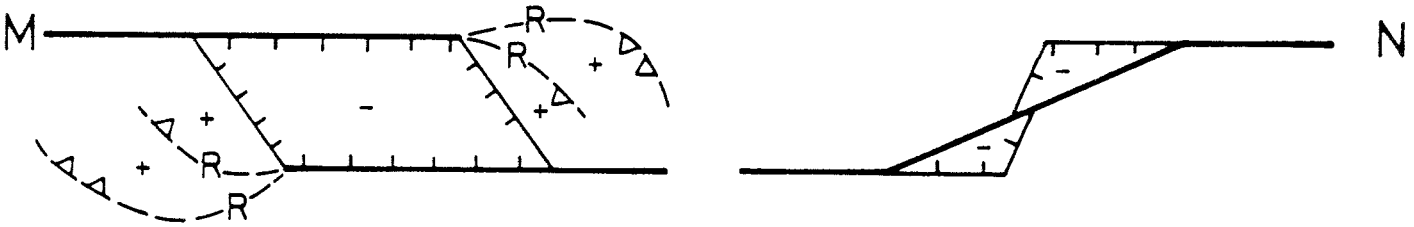

separated angular hills

displaced angular lows

Fig. 19B

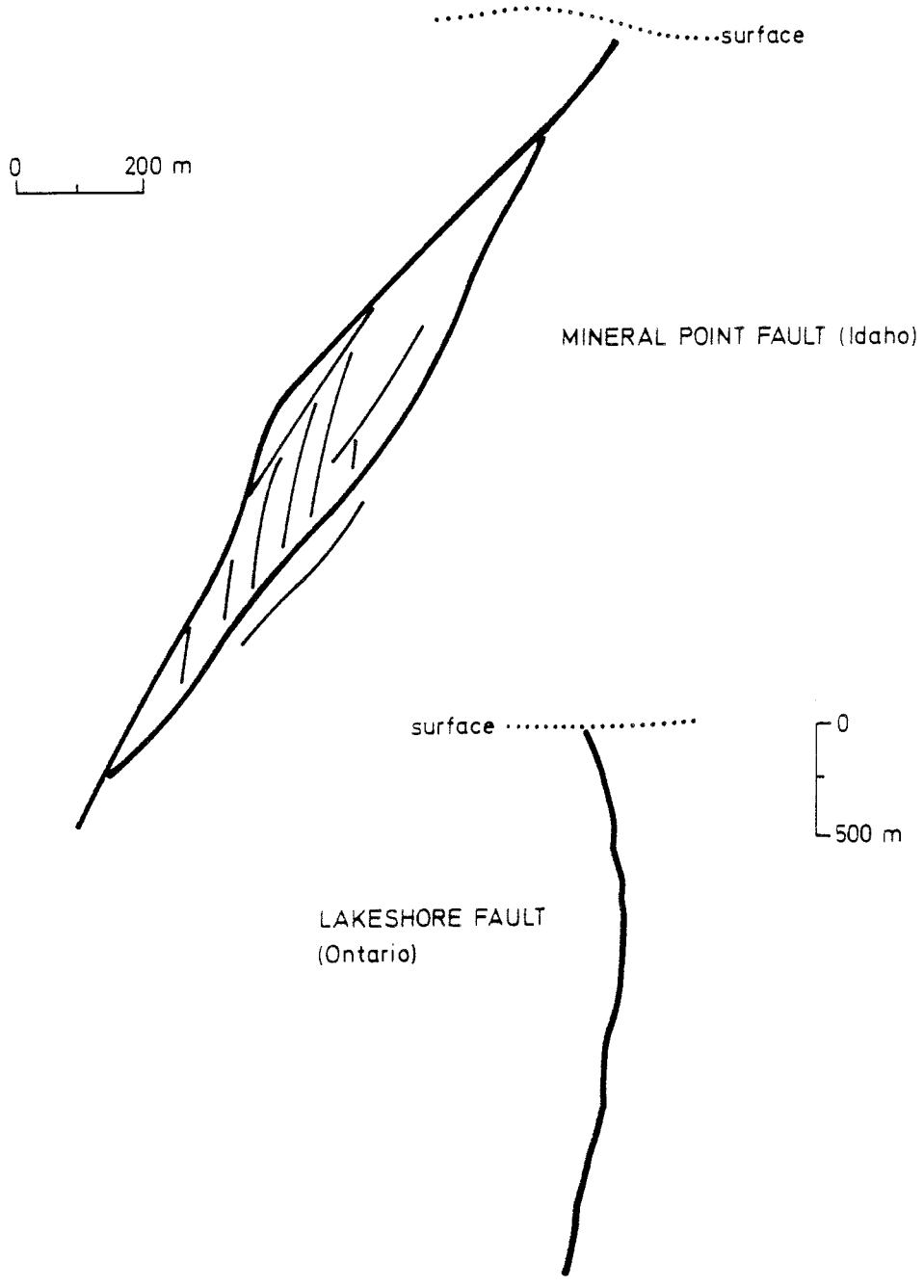

Fig. 20. Vertical sections through faults known from mining. After Wallace and Morris (1979), (1986).

4.2 EXAMPLES FROM ACTIVE FAULT ZONES

Fault zones with large and rapid displacements tend to develop the most obvious patterns of fault induced structures. The San Andreas (and related) fault system is an example of a high speed (about 8 cm a^{-1}) continental plate boundary which has all characteristics of large scale strike--slip associated deformations imprinted on the surrounding crust. The system consists of several major faults (among which the San Andreas FZ is one), each with large displacements and displacement rates (several cm a^{-1}). Considerable mapping has been made along various sections of this fault system. Figure 21 shows an example of a large scale shear lens structure (about 110 x 20 km) mapped by Dibblee (1973) containing thrusted older rock formations along the outer edge. The lens thus once belonged to a shear horst and has subsequently been displaced along the fault. Examples of very long transported lithologies are known along the San Andreas fault zone. In figure 22, two small scale structures typical for strike slip faulting are shown. The Coyote Creek dextral strile slip fault makes a compressional step-over which induced folding in a 7 x 2 km positive shear lens. Lower stratigraphic levels of sediments are exposed in the lens which was expelled by shearing. (Sharp, 1979).

For the Himalayas, where active faulting is induced in the upper crust by plate movements, numerous examples of very recent faulting are demonstrated in Armijo et al. (1986). From this publication, an example of a recent strike slip fault wih tensional step over is shown in figure 19. The step over creates an angular subsidence basin or negative shear lens of about 1 x 1.2 km. The lens is bounded by normal faults and contains a (near) angular lake. The examples of figures 21 and 22 represent 2nd, 3rd, and 4th order shear lenses according to their sizes. Shear basins (pull-apart basins) of larger size are known from many areas and it is very likely that the Precambrian and Paleozoic graben structures in Scandinavia are of similar origin. The Muhos graben in the northern part of the Bay of Bothnia is the nearest known example to the study area.

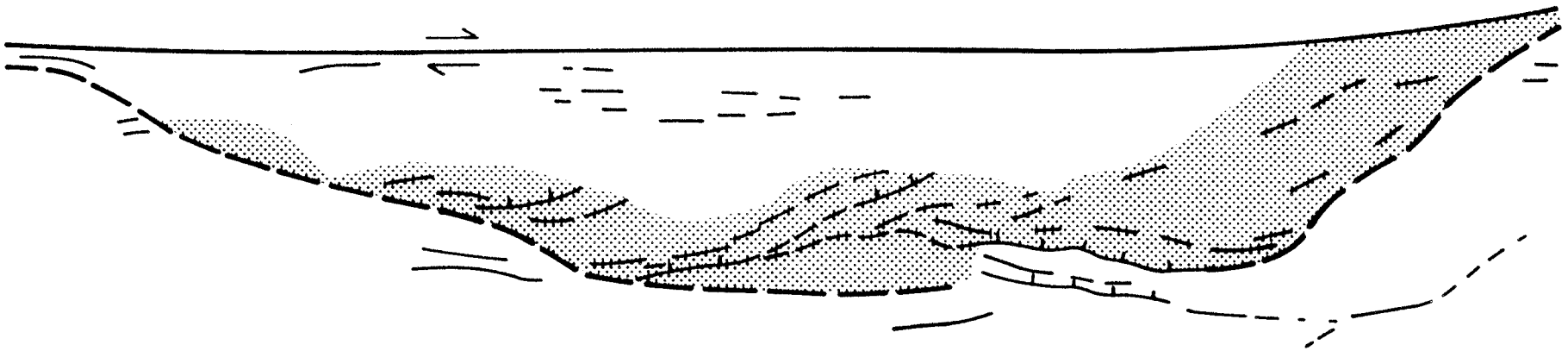

Fig. 21. Part of San Andreas FZ at Carrizo Plain.
Positive shear lens appr 110 km long with older strata exposed in shaded area, trend of fold axes indicated with short lines, thrusts are shown with barbed lines. From Dibblee (1973).

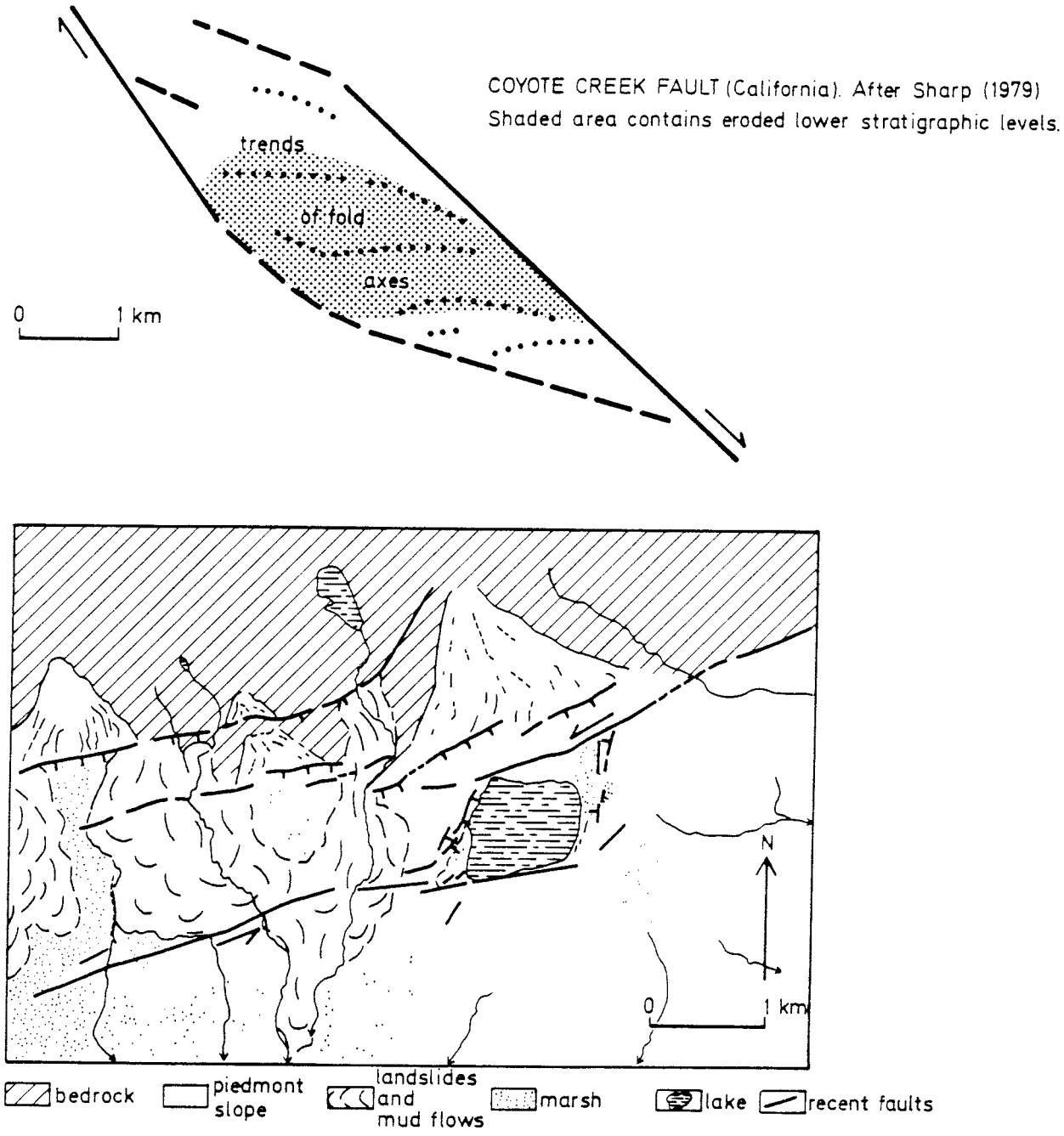

Fig. 22. Examples of shear lenses, positive (compressional) above, from Sharp (1979) and negative (tensional) below, from Armijo et al. (1987). (Himalayas)

5 DISCUSSION

5.1 REGIONAL SETTING

The oldest rocks of the region occur in a small dome of Archean basement in the map area 25 N. The rest of the study area is occupied by rocks which are thought to have been deformed, metamorphosed and intruded during the Svecokarelian orogeny 1.9-1.7 Ga ago (see Geological Map of Northern Fennoscandia, 1986). The area is now dominated by Svecokarelian granitoids. A few dyke swarms of younger Proterozoic age occur and at the southern margin of the area a set of alkaline dykes intruded at -1.1 Ga (Kresten et al. 1977). At the end of the Precambrian, the region was peneplained and outside the study areas, autochthonous Cambrian sediments are preserved. These occur at about 1000 m above sea level at the front of the Caledonian thrust units, about 200 km to the west of the study area and in the Muhos fault graben below sea level, about 50 km to the southeast of the study area. It is likely that the area was again eroded during the Tertiary when the crystalline basement was deeply weathered. Remnants of this weathering may be found locally when protected in downfaulted blocks. Several glaciations in the Quaternary have changed the morphology to its present shape.

Parallel with the rock forming processes, tectonic activity displaced and deformed crustal units. Shortly after the formation of the Svecokarelian crust, Berthelsen and Marker (1986) suggest large scale displacements along strike-slip megashears along N-S lineaments in the Baltic-Bothnian zone and NW-SE lineaments in the Rahe-Ladoga zone. This zone appears about 60 km to the south of the study area and to the east of the Baltic-Bothnian Megashear. On these zones, movements were both sinistral and dextral and resulted in a net 120 to 160 km sinistral displacment along the N-S zone. The existence of late Paleozoic alkaline intrusives at Kalix and Paleozic sediments in the Muhos graben indicate repeated tectonic activity and possible reactivation of the Svecokarelian Megashears.

The plate tectonic situation (fig. 23) indicates a period during the Tertiary, when the regional lineaments again were active. The Senja fracture zone and its fossil trace along the Western Barents Sea continental edge lines up with the Bothnian-Senja system of NW-lineaments through the Lansjärv study area. It is very likely that this zone was active not only just outside Senja at -58 Ma when the first ocean crust of the Atlantic rift formed in the area. In the early stages of the Atlantic opening, the Tertiary fold belt in western Svalbard (Harland 1979) and northeasternmost Greenland (Schack Pedersen and Håkansson 1987) are large scale examples of compressive strike slip block movements. In the western Barents Sea, basin development occurs in late Tertiary times.

Present lithospheric stresses are induced by the plate motion, remaining glacial rebound, and continued changes in plate tectonic patterns. The continued cooling and thickening of the oceanic crust induces flow of mantle material under the continental lithosphere and generates continuous rise and

tilt of the continental edge. Differential opening rates in the Arctic and North Atlantic oceans will induce stresses into the surrounding continental blocks which are likely to be released in existing fault systems. Several 100 km of post glacial fault scarps have been detected in a restricted area between and around the extension of the two large fault zones of the study area - as indicated in figure 10. These mark a late episode of increased tectonic activity of the area. Figure 24 contains an extension south of the study area, showing the location of the Muhos graben.

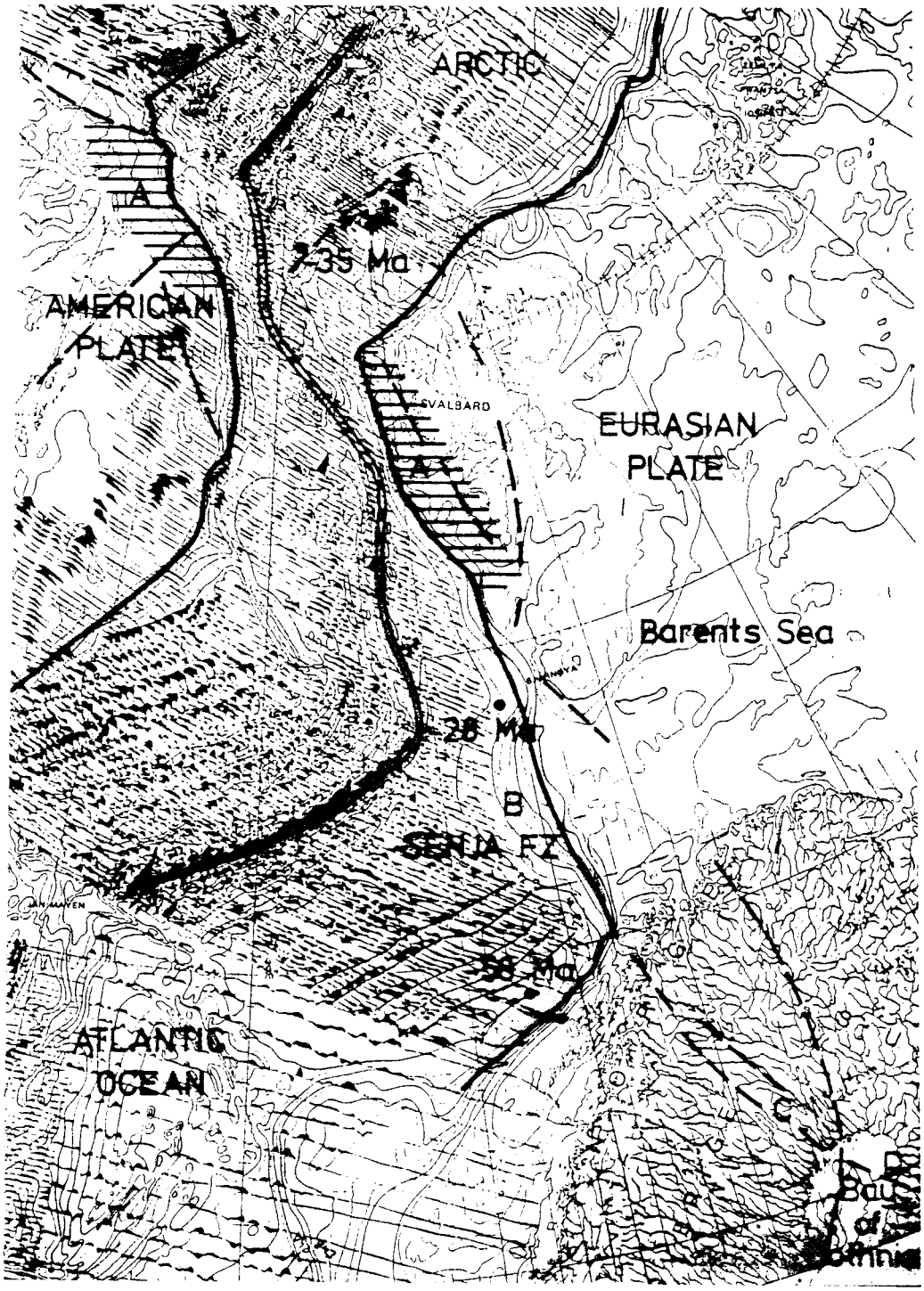

Fig. 23. ═══ Plate boundary in N Atlantic and Arctic oceans ——— approx. edge of continental crust •-58 Ma approx. ages of oceanic crust. ——— Major fault zones. A Displaced Tertiary fold belt, B recent <5 Ma sedimentary loading, C Lansjärv area, D location of Muhos graben (<Paleozoic age). Background map from Kovacs et. al. (1986).

5.2 STRAIN INDICATORS

In the following table, strain indicators have been listed with their approximate ages and method of detection when covered. The strain markers indicate the net accumulated displacement (since their formation) across a fault, or in the case of foliations etc, the general orientation of movements. Reference will be made to some map examples.

strain indicator	age	method	displacement
Svecokarelian rock boundaries	1.6 Ga	magnetic	lateral and vertical
foliations, lineations, mylonites, pseudotachylites	Proterozoic to Tertiary?	bedrock tectonic mapping	horizontal and vertical
dykes	Mid-Proterozoic	magnetic	lateral dominates
Caledonian structures	Mesozoic	bedrock mapping	lateral and/ or vertical
Tertiary land surface	Tertiary	elevation data	vertical and lateral
Striations on fracture fill	Tertiary to present		vertical and lateral
Pre-quaternary weathered rocks	Tertiary	seismic and VLF resistivity	vertical
Quaternary glacial surface	Quaternary	soil mapping excavation	vertical
Erosion surface, shore lines	Post-glacial to recent	levelling	vertical and indirectly lateral
Post glacial sediments	"	soil mapping excavation	vertical
Earth quakes	Present	seismology	
Geodetic networks	"	precision levelling	vertical

With increasing age, more and more complex deformation patterns will be imprinted in fault zones. As erosion progresses, structures of the deeper parts of a zone will be overprinted by structures created in shallower conditions. The most recent fault movements leave imprints in the middle crust and in the most fractured part of the fault. At the surface these imprints will be erased by erosion almost as soon as they form.

Displacements of Svecokarelian rock boundaries are abundant along the NW striking faults of the Bothnian-Senja fault zone. These displacements are often several km both dextral and sinistral. Examples are found in the map area 26 L (aeromagnetic map). Some segments of the larger fault zone show a pronounced cut through strongly parallel foliated rocks. This is especially typical on the N-S trending fault zone segments of the Bothnian-Seiland fault zone. Examples are in the map area 26M (geological map).

Proterozoic dykes (dyke swarms) are seen in several locations (figure 11). The dykes in the block west of the N-S trending Bothnian-Seiland fault zone occur as magnetic slightly arcuate structures cutting Svecocarelian rock boundaries. The dykes indicated in the eastern block are low magnetic and crosscutting. It is unclear if these dyke swarms belong to the same intrusion event. They appear to be cut by some of the major fault zone segments in each of the two steep fault zones. In the western block, the dykes bend when close to the fault zone segments, indicating increasing strain towards the zone. The different parts of the dyke swarms cannot be matched together unless very large displacements are involved (up to 50-100 km). Another interpretation is the formation by en-echelong intrusions during a period of oblique shear stresses.

Caledonian structures (location of autochthonous rocks thrust units) appear displaced along several faults in the area north of Torne Träsk. A total lateral displacement of 30 km can be inferred on 3 faults. More detailed mapping in some critical areas would be necessary for definite calculation of displacements. See map by Gustavsson (1974).

The occurrence of Jotnian sediments in the Muhos Graben about 50 km to the southeast and Cambrian sediments to the south of the study area indicates significant tectonic movement during and after the sedimentation. Further south, large regions of the Bothnian Sea and Bay were also involved. Along the continuation of the westernmost N-S trending lineaments into the Bay of Bothnia (and just south of the study area), a distinct step in the bottom morphology of about 50 m indicates where Jotnian and Cambrian sediments are downfaulted to the east.

The Tertiary land surface remained after the erosion of paleozoic sediments. Most morphologic features in the study area are likely to be remnants of this surface. Displacements of such features are seen along several of the major fault zone segments. In the map area 26L, the NW-trending Vuotta fault zone segment and the N-trending Kalix älv fault zone segment have distinct displacement features. (See elevation relief maps). The elevation data show a pronounced horst or rise NE of the Lule Älv fault zone segment. In the Tertiary a new plate boundary formed just off the Norwegian coast at Senja and the NW-trending fault zone acted as transform fault between the Atlantic and the Arctic rifts.

As shown previously, active strike slip faults will induce considerable vertical displacements and changes in the morphology where they curve. When these displacements are

faster than erosion, a net contribution will accumulate in the morphology. The simple relation between fault displacement and shear lens subsidence in chapter 4.1 indicates that a fault displacement of 1 mm a^{-1} will induce a subsidence of 1 mm a^{-1} in a basin which is twice as deep as it is wide and has a triangular cross section. In 10^4 years, up to 10 m subsidence will have occurred. This simple relation can be used as first approximation of strain rates when the dimensions and age of a subsidence basin are known.

Quaternary sediments and shore lines are strain indicators for the most recent fault movements. The post glacial faults were first detected because of their conspicious redistribution of the moraine layers. Other structures which also would be indicative of fault movements and which are observed on earth quake ruptures at the surface have not yet been looked for in a systematic way. Such structures are wrinkle ridges, tension cracks in addition to the mentioned shear lenses. Precise levelling and dating of shore lines would also reveal any fault induced displacements.

Precise levelling along roads would indicate the vertical component of any current movements.

Fig. 25-27 show structures interpreted as indicative of rather recent displacements. Full lines represent regional fault zone segments determined by aeromagnetic interpretation. Broken lines represent local faults interpreted from photography. The precise ages of such structures are however unknown.

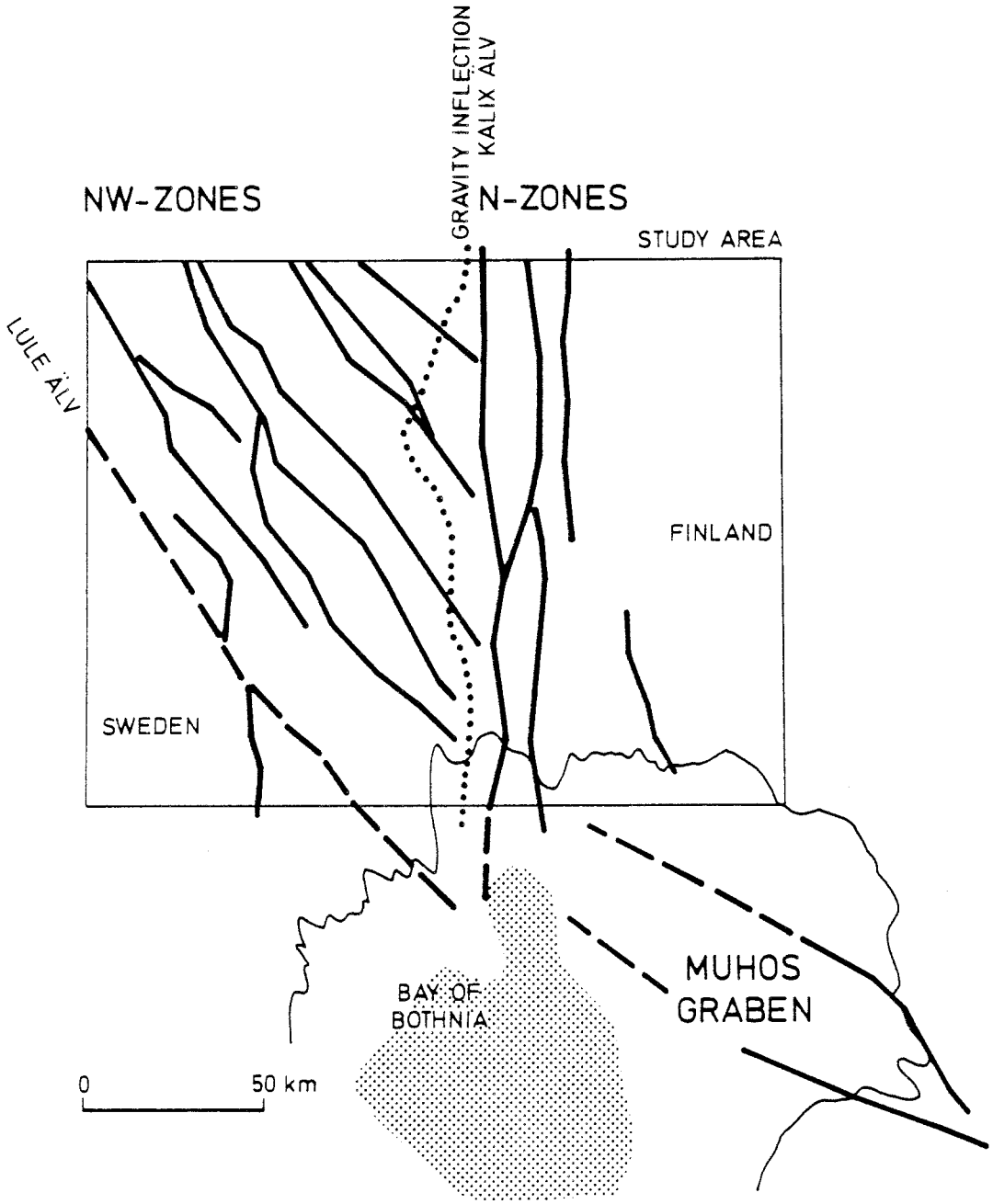

Fig. 24. Major fault zones in study area and location of Muhos Graben. (Jotnian sediments). Cambrian sediments occur just west of the graben (shaded) (Ahlberg 1986).

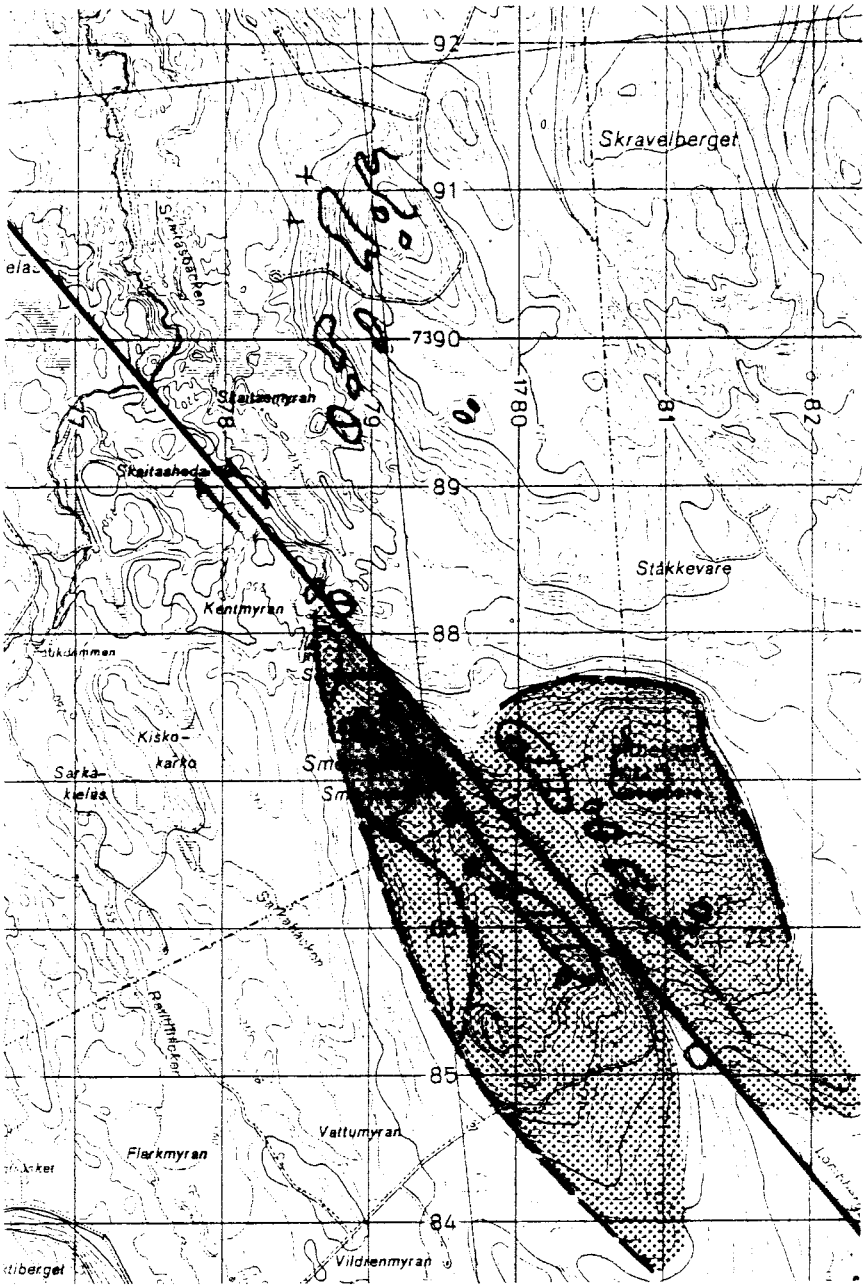

Fig. 25. The Vitberget displaced 4th order positive shear lens (shaded). Map area 26L 7g. Grid size 1×1 km.

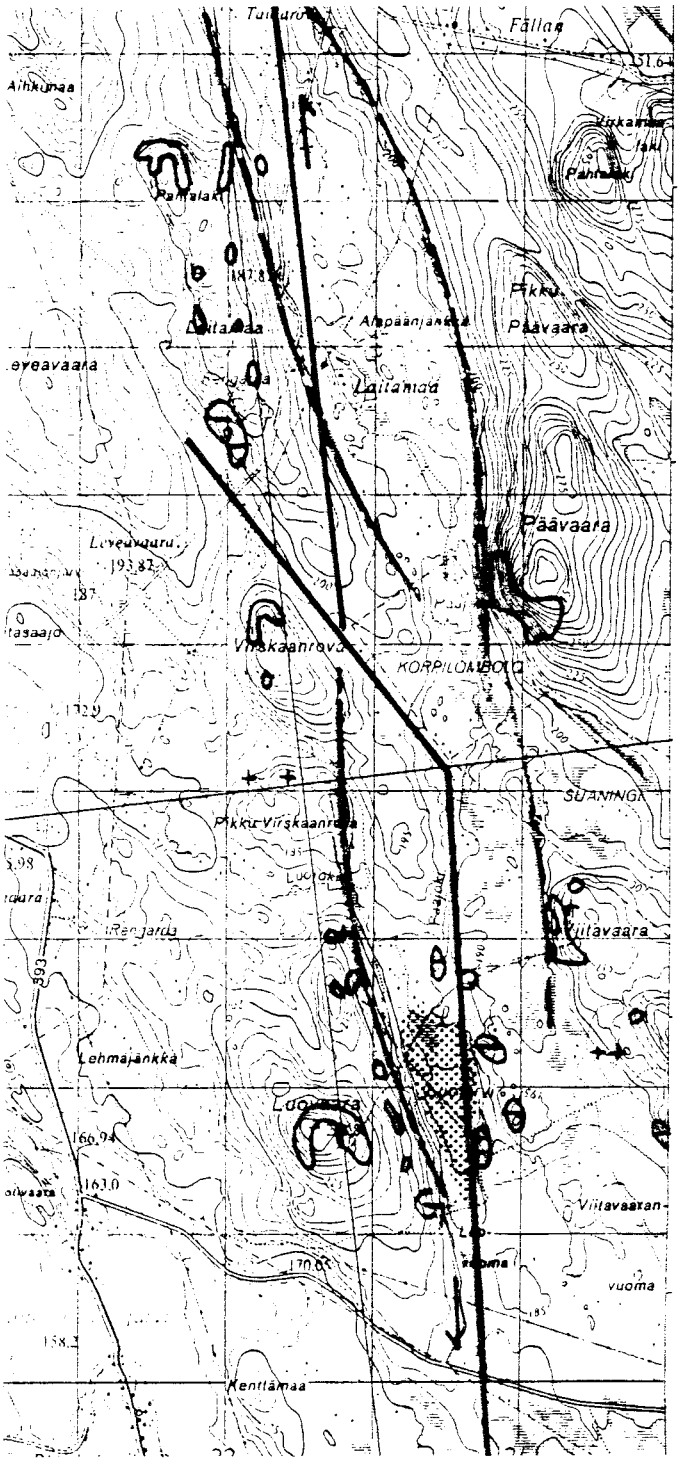

Fig. 26. The Luojärvi 4th order negative shear lens (shaded). Map area 27M 7e. Grid size 1×1 km.

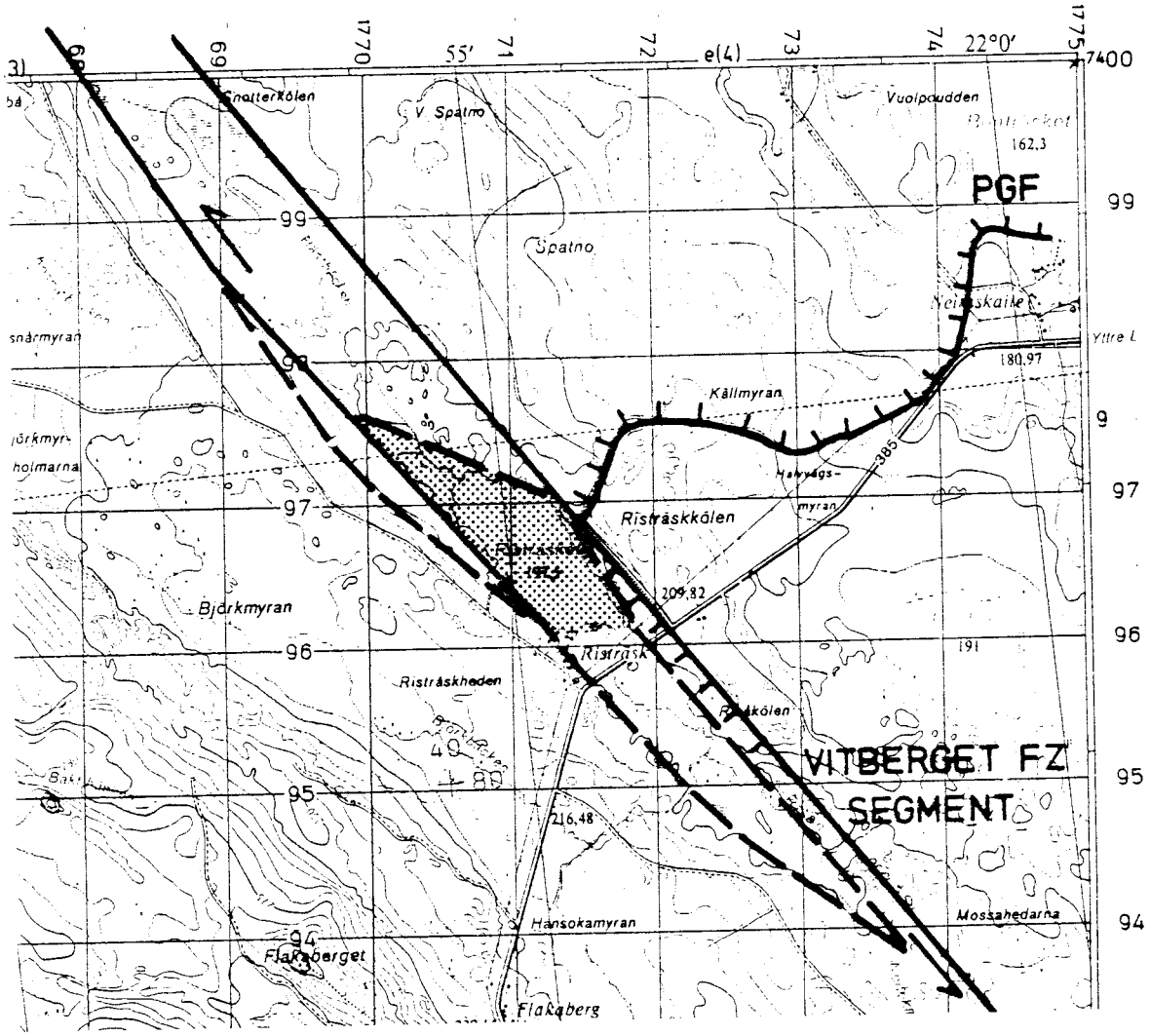

Fig. 27. The Risträsket 4th order negative shear lens (shaded) and the Risträskkölen PGF thrust flake. Map area 26L 4e. Grid size 1×1 km.

5.3 ESTIMATED STRAIN RATES

In the following table, estimated minimum averaged to present strain rates are listed. They have been computed from total displacements across a fault zone or a single fault.

time	1.5 Ga	500 Ma	200 Ma	50 Ma	8 ka	present
displacement	30 km	30 km	>200 km	1.6 km	10-2 m	
nr of faults	4	3	4	1	1	
rate mm a^{-1}	0.005	0.02	>0.25	0.03	0.6-0.1	0.1
structure	NW and N zones Sveco-karelian rocks	Caledonian front	Devonian Svalbard	Vitberget pos. shear lens	Risträsk Luojärvi neg. shear lenses	earth quakes SW Sweden
reference other than this report	Berthelsen and Marker (1986)	Map by Gustavsson (1974)	Harland (1979)			Slunga (1985)

The rather low strain rates for the older structures represent the absolute minimum required to accumulate the inferred displacements. If the time intervals for the actual movements are restricted, very much larger strain rates have to occur. Thus, the displacements along the Senja transform fault are likely to have occurred in the time interval -58 Ma to -28 Ma which results in a total strain rate of about 1.2 cm a^{-1} or 3 mm a^{-1} if spread on 4 faults (the total displacement being about 450 km). See reconstruction of Arctic ocean surroundings in Kovacs et al. (1986). Such high strain rates are also likely to have occurred in the Precambrian on the N-S fault zone at least (Berthelsen and Marker, 1986). The recent strain rates can be more constrained when more detailed information becomes available on the nature and age of small subsidence structures, and when the earth quake activity is analyzed during a longer time interval (as in SW Sweden for example, Slunga, 1985). Figures of the estimated order of magnitude, i.e. 0.1-1 mm a^{-1}, are indicative of the ongoing deformation in the uppermost crust due to tectonic forces. Extra stresses created by deglaciation unloading of the crust may locally add another 0.5 mm a^{-1} to the average strain rate (if the PGF scarps represent an accumulated displacement).

The Vitberget, Luojärvi and Risträsket shear lenses are shown in figures 25-27.

5.4 TENTATIVE MODEL(S) FOR THE ONGOING TECTONIC DEFORMATION

Based on the interpretation of the geophysical and terrain elevation data combined with indications of differential land uplift and small scale shear lens formation, the following

tentative model for the present tectonic deformation will be presented and shortly discussed. This model(s) must be confirmed by further research and mapping of deformation structures resulting from relatively small strain rates. The driving forces are plate tectonic - the Eurasian plate moves at cm a^{-1} rates away from the Atlantic and Arctic rifts. The resulting strain is concentrated to the lithosphere. To accommodate internal deformation, the continental part of the plate responds with activation of existing weak zones in its brittle parts and flow in its ductile parts. The two regional fault zones observed in the study area act as the release structures in the upper crust for stresses induced by the differential plate motion 150 km below. Stress induced by ridge push about 1000 km to 1500 km away may contribute as it has been calculated as concentrating to the upper crust within 10 Ma (Hasegawa et al. 1985). See also discussion of these problems in Stephansson (1987).

The drastic sinistral transform displacement of the Atlantic rift to the Arctic rift which started along the Senja fracture zone at -58 Ma, is likely to have reactivated adjacent continental fractures. Differential opening rates in the two rift segments across the transform will induce a continuous deformation of parts of the adjoining plates. Changes of these conditions with time will cause shifts in the relative motions of crustal blocks.

Seen from the Lansjärv area and its nearest surroundings, the existence and function of the two steep N and NW trending fault zones can be interpreted in three ways:

1. as a set of conjugate shear faults with NNW-SSE compression when the majority of block movement indications are considered,

2. as a compressional (retarding) step-over of the Bothnian--Senja shear zone with NE-Sw compression when both N and NW faults have dextral sense of displacement,

3. as a tensional (releasing) step-over of the Bothnian--Seiland shear zone with NE-SW extension when both N and NW zones have sinistral sense of displacement.

The three alternatives are illustrated in figure 28. It is quite possible that all three activities occurred during the last 60 Ma. The following table compares the model requirements with inferred movements.

model	model requirements sense of movements on		N block between NW and N zones	intersection area between NW and N zones
	NW zones	N zones		
1	dextral	sinistral	up	down
2	dextral	dextral	up	up
3	sinistral	sinistral	down	down
inferred	dextral and sinistral	sinistral	up	down

As can be seen, no unique combination of tendencies is clear yet mainly because of difficulties in precise correlation in time of the various deformations. If the inferred dextral displacements on the NW zones together with the rise of the N block between N and NW fault zones are relatively older, than the occurrence of sinistral younger displacements on NW zones indicates a change from model 2 towards model 3.

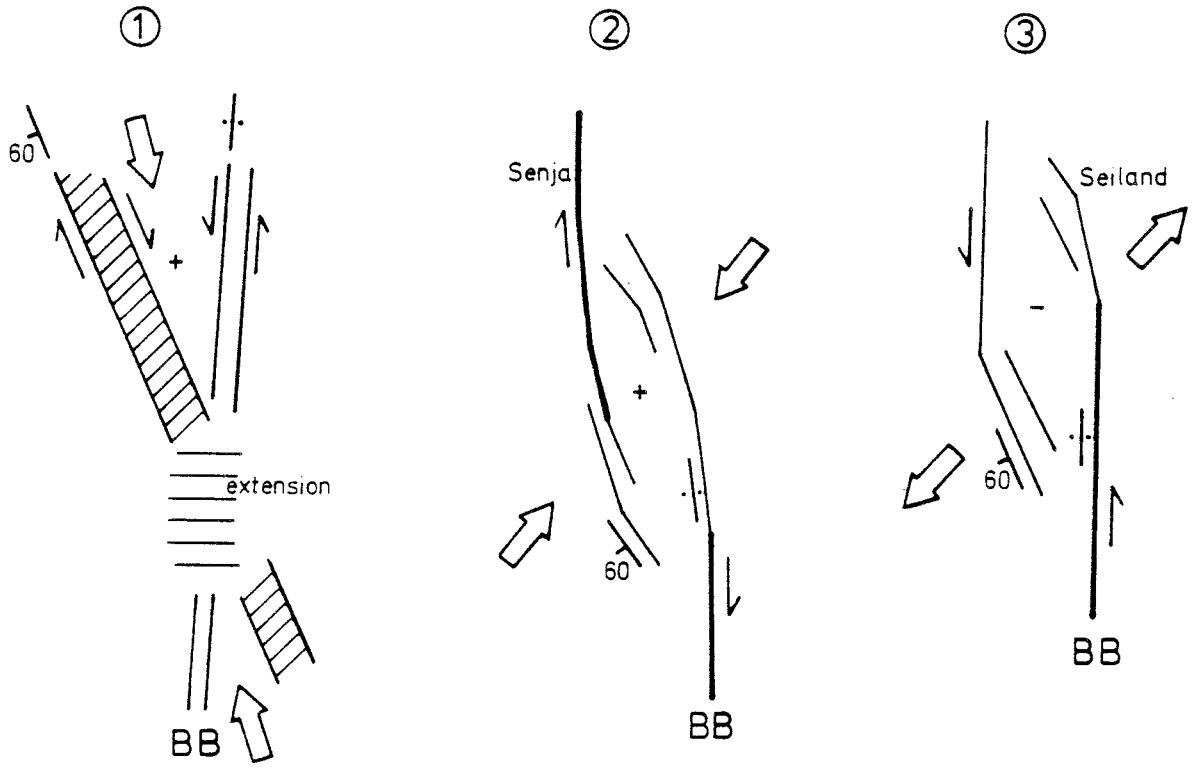

Fig. 28. Three models for present block movements. The inferred movements in the Lansjärv area are not yet conclusive to any model. BB=Baltic-Bothnian Mega shear.

5.5 ESTIMATES OF THE SENSE OF RECENT BLOCK MOVEMENTS

The smallest shear lenses reflect the most recent block movements. In the Tectonic Interpretation Map, an attempt has been made to classify the shear lenses of approximately 3rd order magnitude into positive (compressional) or negative (tensional) due to their topographic relief. Only a few of

these lenses are decisive and in two fault zones contradictional senses of movement were obtained. On the NW fault zones, 10 indications of dextral strike slip movements can be inferred (including all the major fault zone segments). Two cases of sinistral displacement were found, the Telmberget 3rd order positive shear lens (fig. 12) and the Risträsket 4th order negative shear lense, shown in figure 27. On the N-fault zones, 5 indications of sinistral, strike-slip movements can be inferred, including two of the major fault zones. No cases of dextral displacement were found. The Luojärvi 4th order negative shear lens is shown in figure 25. As the interpretations were made on a regional scale, the indications should be field controlled in order to more precisely locate the main fault and if possible to determine the character of the shear lens deformation. The locations of the shear lenses used for the determination of the sense of fault movement are listed below.

fault zone segment	location map area code	type of indication	sense of displacement	reference to fig.
NW zone	25-26 K 7-1 e-i	large neg. lens at bend of Lule Älv fault zone	D	
"	27 K 5 h	displ. of pos. lenses	D	
" B	27 K 5 j	pos. lens at stepover	D	
" G	27 L 8 b	neg. lens at stepover	D	
" C	27 L 8 h	neg. lens at stepover	D	
" C	27 L 4 g	neg. lens at stepover	D	
" G	27 L 3 g	pos. lens at stepover	S	fig. 12
" B	26 L 9 e	neg. lens at stepover	S	fig. 27
" B	26 L 7 g	displ. of pos. lens	D	fig. 25
" F	26 L 3 b	neg. lens at stepover	D	
" A	26 L 2-3 f-g	pos. lenses at bend	D	
" B	26 L 1 j	neg. lens at stepover	D	
N zone	25-26 M 9-0 c	neg. lens at stepover	S	
" D	26 M 6 c	neg. lens at stepover	S	
" D	27 M 1 b	neg. lens at bend	S	
" D	27 M 6 b	neg. lens at stepover	S	
" E	27 M 7 e	neg. lens at stepover	S	fig. 26

The positive shear lenses which have no well defined step--over or curvature are inconclusive regarding the direction

of displacement. More precise interpretations of detailed data would in some cases allow a more decisive interpretation. As the topographic relief is assumed to represent the combined result from erosion and fault movements, it is not always clear how to separate the two factors. A positive relief will remain as erosion cuts deeper in surrounding fault zones. This relief can, however, be maintained and enhanced by fault movements if a bend or step-over occurs. Similarly, a negative relief will result from the existence of a fault zone as erosion can act faster in fractured zones. In negative shear lenses, this tendency will be further enhanced as these tend to be more fractured and fill with sediments. Again the configuration of the bounding faults indicate fault movements which can maintain and enhance the relief.

5.6 SITES FOR DRILLING AND DEFORMATION MEASUREMENTS

For geodetic (distance and triangulation) measurements of present block movements, a stable foundation of observation points is an important prerequisite. To obtain maximum resolution of the measurements, short distances between observation points is the second prerequisite. the third is there are indications of possible movements. By studying the outcrop maps (report by Sundh and Wahlroos, 1987), three locations were selected for further field control. These locations were all on fault zone segments with distinct morphologic depressions implying relatively recent enhancement by erosion and/or block movements. The location at the Vitberget fault zone segment was also close to the steep sidewall of the postglacially active Risträskkölen thrust flake. On field examination, two sites are proposed for further studies with geodetic measurements of displacements. These are the Vitberget 4th order positive shear lens which is possibly displaced by later block movements, and the Luojärvi 4th order negative shear lens. The locations are on a NW and N-trending fault zone segment respectively. The third location at Rödstenshuvudet is also qualified and has a rather dramatic relied and complex topography. The three localities are shown with maps in figure 29. Lines short enough for maximum resolution could not be found in any location. Instead the time interval covered must be extended. In connection with the geodetic observations, a precise mapping with geophysical methods of the location of the actual faults would be necessary.

observation site name	location on map area	type of structure	fault	minimum distance between outcrops across fault
Vitberget	26 L 7 f	displaced pos. lens	(NW) B	350 m
Luojärvi	27 M j7 e	neg. lens	(N) E	400 m
Rödstenshuvudet	26 L 1 c	complex	(NW) A	300 m

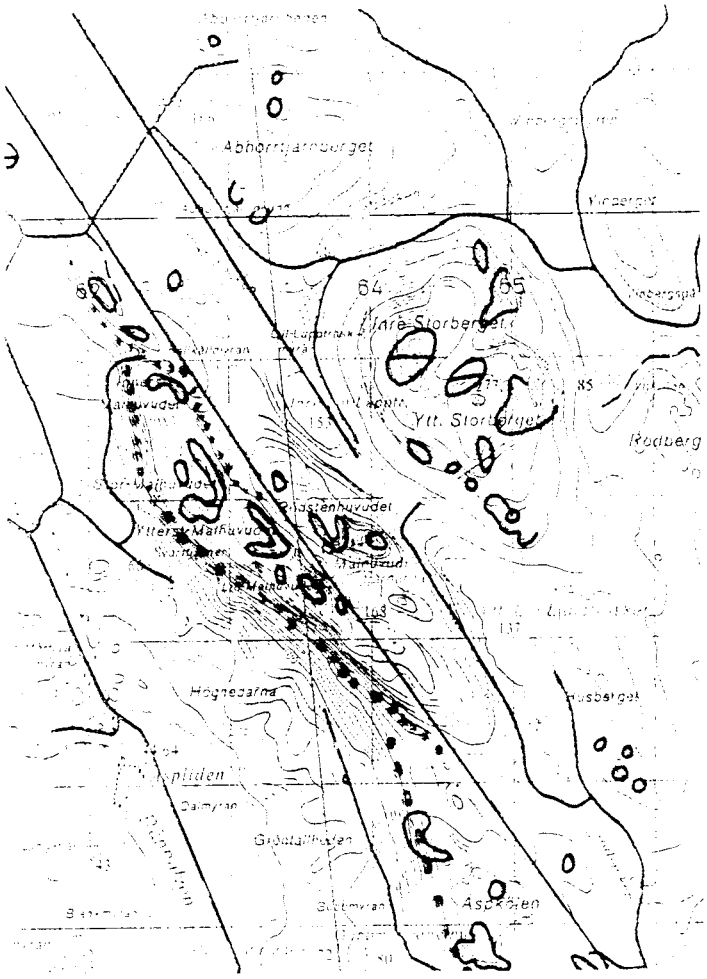

A

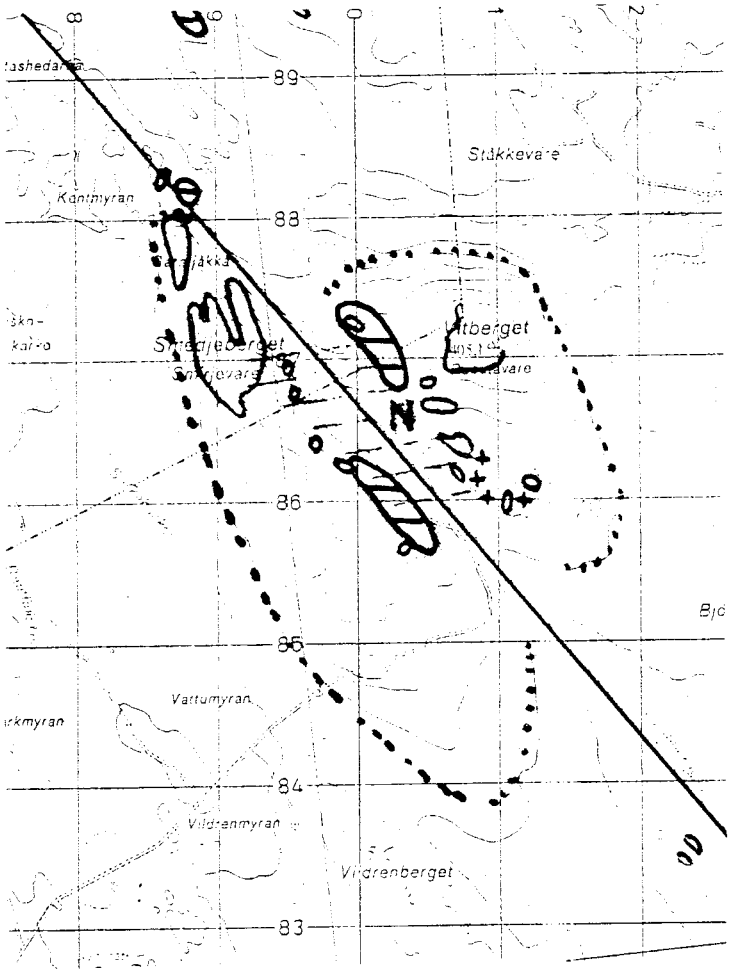

B

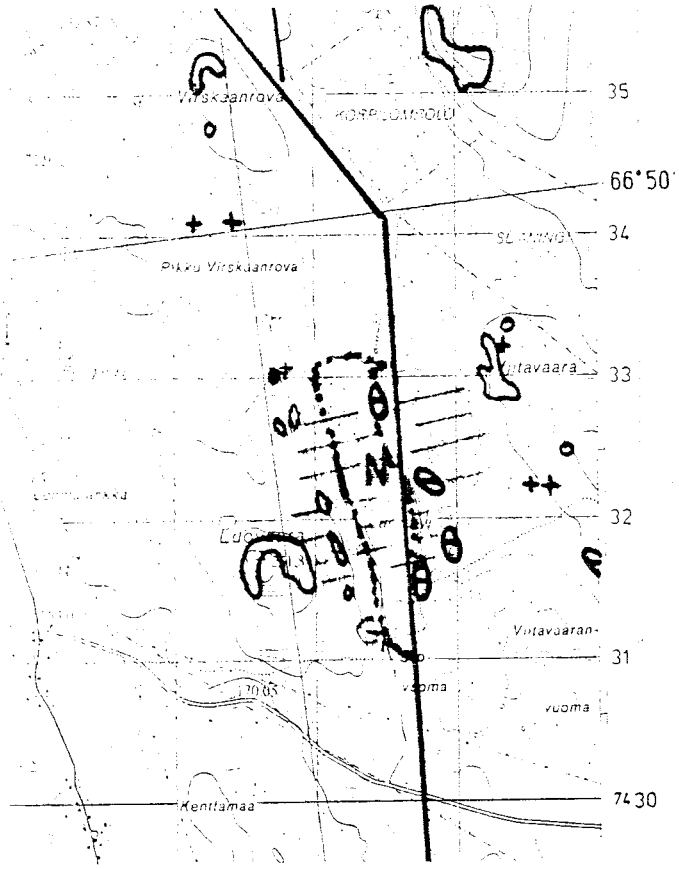

C

Fig. 29. Location of suggested geodetic networks (N).
A Rödstenshuvudet (fault zone A) map area 26L 1c, B Vitberget (fault zone B) map area 26L 7f, C Luojärvi (fault zone E) map area 27M 7e. Heavy lines show fault zone location. Heavy contours indicate areas with outcropping bedrock. Dotted lines indicate local shear lens.

The selection of a drill site, where the PGF and parts of the low angle NNE-trending faults could be drilled, was based on the dip estimates of the low angle branch of the PGF at Mäjärvberget. Stratum contours for the fault surface could be constructed for a short segment of the fault. The extrapolated dip predicts the PGF at 150 m in a location 1 km behind the fault scarp close to the road between Lansjärv and Ängesså. Figure 12 shows the proposed location. As it is within the 3rd order positive shear lens of Telmberget, considerable fracturing may occur. The dips of two NW-trending faults within 200 m of the drill site are not known.

6. CONCLUSIONS

For this study, the results from the Nordkalott project which for the first time produced an anlysis of fault zones in a large region of the Fennoscandian shield, were used to define a critical area for possible recent crustal deformations. Several distinct systems of faults could be identified setting a regional framework to the study area around Lansjärv. Close structural connections with the recent (less than 60 Ma) plate tectonic situation are apparent as one major fault system is the strike continuation of the Senja Fracture Zone into the continental crust against which the oceanic crust terminates and the active Atlantic oceanic rift steps to the active Arctic oceanic rift. Plate spreading at different segments of the rift system could induce stresses in the continental crust. This deformation is interpreted to occur mainly connected to one or several lithospheric lenses surrounded by systems of pronounced fault zones. The Senja lens has a slightly higher elevation than its surroundings. This together with the shape of the lens suggest an ongoing transpressional slip. In the Lansjärv area, the NW and N fault zones appear as very sharp, about 200 m wide, magnetic low lineaments with associated large lateral displacements of magnetic reference structures. Many drastic changes in the bedrock lithology occur along these lineaments. Single fault zones in each system represent, on average, 200 m wide, movement zones, interconnected in an elongate lens like pattern.

For the first time, dips of fault zones have been calculated using ground and airborne magnetic and electromagnetic data. The dips of these zones are steep at the surface but may flatten at depth. Close to each movement zone, series of shear lenses, several km wide, can be seen cutting off arcuate segments of the surroundings. The width of these shear lens patterns grades into the size of the network. The shear lenses surrounding the fault zones may account for associated gravity lows following the strike direction of several fault zones as the 200 m wide zones themselves are too small to create gravity anomalies.

At outcrops close to the major fault zones, a variety of strain indicators ranging from ductile to brittle deformation show that these faults have been active in very different crustal depth regimes over a very long period of time. The most recent (post-glacial) faults were detected and described

by Lagerbäck (1979) and Kujansuu (1972). Today, several 100 km of PGF fault scarps are known in northern Scandinavia. Most of them have NNE strike directions and are scarps of steep to gentle SE dipping faults. They typically occur between the NW striking major fault zones and seem to be closely related to a set of low angle movement zones. These close spatial and structural relations to the NW zones suggest simultaneous activity along linked faults (Henkel et al. 1983). The same can be suspected for the N faults. A few indications of PGF scarps along single faults of both the N and NW steep as well as the gently dipping NNE regional fault systems improve this hypothesis. These features need a more detailed study in order to ensure their post-glacial nature. In Henkel and Wållberg (1987), a detailed study of the relations between sections of the PGF and local and regional faults is made. Study of digital elevation data in the Lansjärv region has added further improvements to the tectonic concept. The distinct imprint of fault zones and fault movements on the morphology of the study area indicates strong activity along the three regional fault systems. One very important effect is the formation of topographically positive and negative shear lenses where steps or bends in the regional fault zones create structures which can release compressional or tensional stresses. The PGF scarps usually stop along the border to such lenses, indicating that they deformed simultaneously with the post-glacial fault movement.

Stress occurs around several boundaries of each shear lens at the same time. All stages of deformation can be observed ranging from small (0.2 x 2 km) recent and sharply developed basins and horsts to very elongated narrow, grabenlike structures and displaced or sliced horsts. A rough estimation of the response of the free surface to a continuous strike slip movement of 1 mm a^{-1} results in an adjustment of the horizontal surface of about 2 m in a period of 8000 years. Such figures appear to be in the correct order of magnitude judging from the depths of the smallest shear basins.

Two other features deserve attention. 1) Several, on average 15x5 km, north-south oriented areas with pronounced elevation appear not to be positive shear lenses (as they are not surrounded by major fault zones). 2) A series of northwest--southeast oriented topographic lows between major N-S lineaments are unlikely to be negative shear lenses. These features are tentatively interpreted as compressional and tensional features respectively. Profile A and J in report by Henkel (1987) show examples of these types of structures.

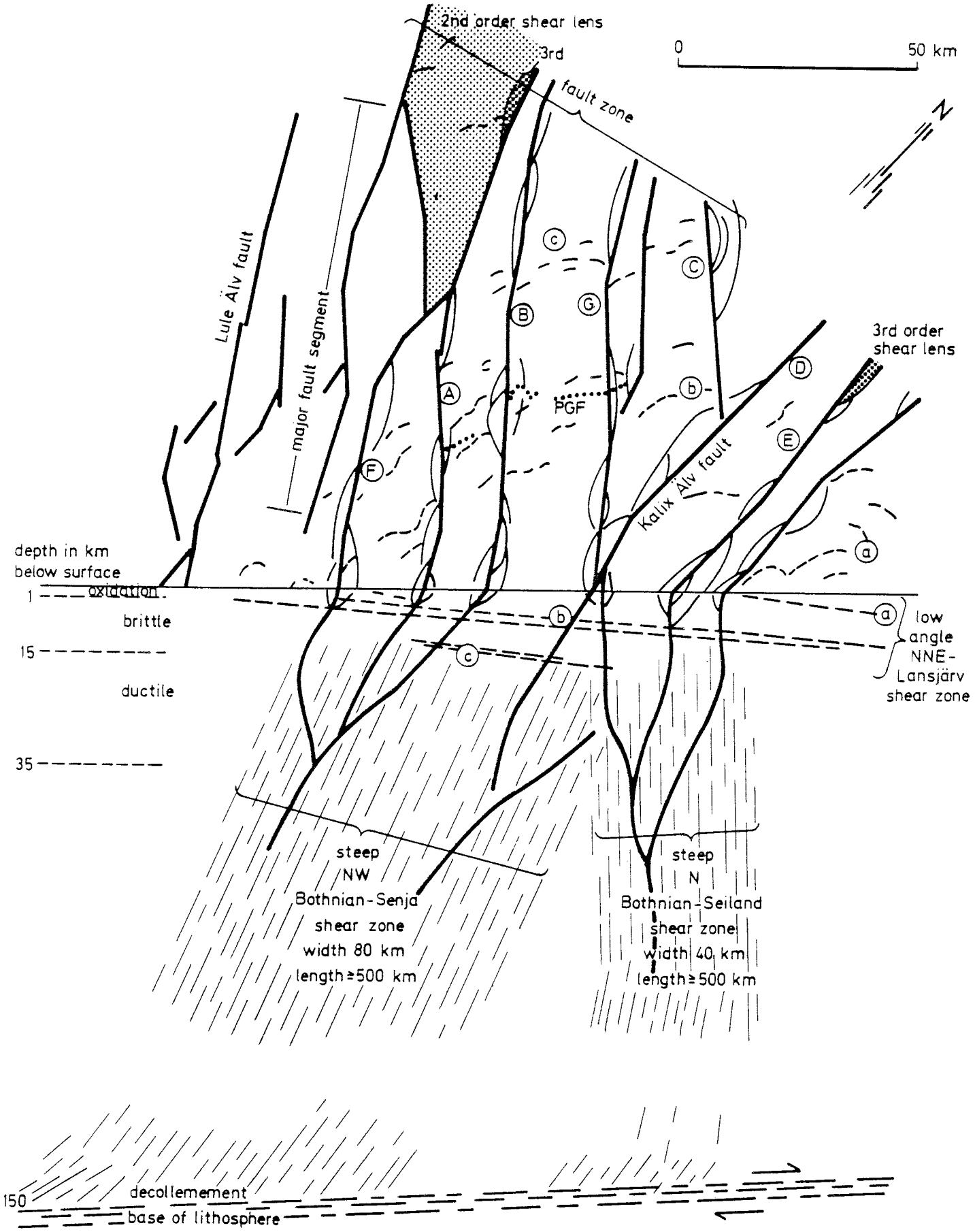

Fig. 30. Block diagram showing lithosphere section SW-NE through the Lansjärv study area. A-G and a-c refer to fault zones treated in the text.

CONCLUSIONS TECTONIC PATTERNS

The following conclusions can summarize the tectonic patterns; see also fig. 30.

- The Lansjärv region is situated at the southern extremity of a 600 x 200 km, tectonic lens (the Senja Lens).

- The southern end of the Senja lens is limited by two sets of regional fault systems striking NW and N and has about 50 m increased elevation.

- The lens may represent a compressional lithospheric structure.

- The single larger faults of each set are connected in a network of smaller lenses showing locally both compressional and tensional features.

- Major single faults of the N and NW system are about 200 m wide and have general steep dips.

- NW zones dip generally 60 degrees to the SW.

- N zones dip generally steeply (>70°) to the W.

- NNE gently dipping zones (less than 5 degrees) are a few 100 m wide; the width of single faults is not known,

- each steep fault zone is surrounded by a several km wide series of smaller shear lenses,

- the outer faults bounding the shear lenses are less likely to be as steep as the main fault.

- the interior of lenses between major fault zones are less affected by fault deformation compared to the main zones,

- negative shear lenses are likely to be more brecciated than positive (Sibson 1986).

- the criteria so far cited define a pattern typical for a strike slip fault zone of lithospheric dimensions.

- the post glacial fault scarps may represent movements of flat lying fault system and the interaction with the free surface,

- several other morphologic features can be interpreted as effects of post glacial strike slip movements (i.e. small scarps, horsts, basins etc.),

The Lule älv NW fault (zone) and a NW zone in the map area 25M have no (or very minor) magnetic dislocations.

CONCLUSIONS METHODS

- Aeromagnetic measurements provide the best indicator of large fault zones (width >50 m, length >5 km) with steep dips.

- Detailed ground geophysical measurements with VLF and slingram are necessary for the detection of smaller scale fault features,

- ground radar measurements could be used for precise location of buried fault scarps,

- in combination with aeromagnetic measurements, terrain elevation data give an enhanced interpretation of fault mechanisms,

- elevation data have been most effective in locating scarps of gently dipping zones,

- a sufficiently large study area is necessary to understand local features of faulting.

Improvement of methods

- Reflection seismic methods in connection with slingram should be developed for all fault geometries but especially the flat lying faults.

- direct analytical tools in the image analyzing system need to be developed for fault and fault related structural classification.

DIRECT MEASUREMENTS OF BLOCK MOVEMENTS IN SELECTED AREAS

For this purpose several sites along major faults have been field checked with respect to feasibility of establishing geodetic networks. Two sites appear useful at Vitberget (NW fault zone) and Luojärvi (N-fault zone) - for location refer to main map.

REGISTRATION AND LOCATION OF SEISMIC EVENTS IN THE ENTIRE AREA

For this purpose two seismic networks are established and run by FOA and the Seismological Institution at the University of Uppsala.

DEFORMATION PATTERNS IN QUATERNARY DEPOSITS

Excavations for this purpose are planned on PGF scarps and in surrounding locations. Particular attention should ge given to glacial and post-glacial deposits in the N and NW lineaments.

NEW FRACTURING

So far, no case of post-glacial fracturing in the bedrock has been observed; which does not exclude their existence. In southern Sweden a few cases of strong, apparently recent fracturing of surface rocks have been noticed and are documented in Agrell (1984). The relation of these cases with tectonic patterns of the area is however unknown. The occurrence of distinct post-glacial scarps and the displacements of Quaternary deposits indicate considerable block movements in the order up to tens of meters in the last 8000 years. The well developed fault systems of the area can accommodate most of the strain (especially at low strain rates) without fracturing, except in extreme situations. Some rock volumes are however in a position where new fracturing is likely to occur:

- the wedge between the free surface and a (re)activated gently dipping fault(zone),

- the block between the faults in a tensional step over (shear basin),

- the hanging wall block adjacent to a tensional bend in a main fault zone. The drilling at the northern Lansjärv PGF segment is located in a wedge overlying the extrapolated location of the PGF surface. The other situations could also be tested by drilling in suitable structures.

ACKNOWLEDGEMENTS

Inspiring discussions with Christopher Talbot, Richard Sibson, Allan Lindh and Thomas Sjöstrand are highly appreciated. I also want to acknowledge the stimulating feed back from the SKB reference group. Without the engagement and cooperation of all the listed participants, this work would not have been accomplished.

REFERENCES

Agrell. H., 1984: Dokumentationsrapport över urbergsgrottan Gillberga gryt, Trollegatar m.fl. strukturer. Sveriges Geologiska Undersökning.

Ahlberg, P., 1986: Berggrunden på kontinentsockeln. Sveriges Geologiska Undersökning, Rapporter och meddelanden nr 47.

Arkko. V., 1986: The Nordkalott projekt - model calculations of magnetic and gravimetric data. SGU BRAP 86409.

Arkko, V. and Lind, J., 1988: SKB projekt bergets stabilitet, Tektoniska studier i Lansjärv. Lägesrapport över kompletterande markgeofysikmätningar. SKB AR 88-03.

Arkko, V., 1988: SKB projekt bergets stabilitet, Tektoniska studier i Lansjärv. Report of the magnetic dip determinations. SKB AR 88-04.

Armijo, R., Tapponier, P., Mercier, J.L., Tong-Lin, H., 1986: Quaternary extension in southern Tibet: Field observations and tectonic implications. Journ. of Geophysical Research. Vol 9 No 814.

Berthelsen, A., and Marker, M., 1986: 1.9-1.8 Ga old strike slip megashears in the Baltic shield and their plate tectonic implications. Tectonophysics 128 pp 163-181.

Brun, J.P., and Cobbold, P.R., 1980: Strain heating and thermal softening in continental shear zones: A review. Journal of Structural Geology, Vol 2 Pt 1-2, pp 149-158.

Deng, Q., Wu, D., Zhang, P., and Chen,S., 1986: Structure and deformational character of strike slip fault zones. PAGEOPH 124, Pt 1-2, pp 203-223.

Dibblee, T.W. Jr., 1973: Regional geological maps of San Andreas and related faults in Carrizo Plain etc. US Geological Survey Miscellaneous Geologic Investigations, Map I-757.

Elvehage, Chr., and Andersson, P., 1986: The use of elevation data bases in computer assisted cartography. National Land Survey of Sweden. Professional Papers. Report 1986:17.

Gustavsson, M., 1974: Berggrundskart Narvik 1:250 000. Norges Geologiske Undersøkelse.

Hanks, C.Th., 1979: Seismic width of active crustal fault zones. In: Proceedings of Conference VIII Analysis of fault zones in bedrock. US Geological Survey Open File Report 79-1239.

Harland, W.B., 1979: A review of major fault zones in Svalbard. In Proceedings of Conference VIII. Analysis of actual fault zones in bedrock. US Geological Survey. Open file Report 79-1239.

Hasegawa, H.S., Adams, J., and Yamazadiki, K., 1985: Upper crustal stresses and vertical stress migration in eastern Canada. J. Geoph. Res. Vol 90 pp 3637-3648.

Henkel, H., 1986: Aeromagnetic Interpretation Map of Northern Fennoscandia. Geological Surveys of Finland, Norway, and Sweden. ISBN 91-7158-376-9.

Henkel, H., and Guzmán, M., 1977: Magnetic features of fracture zones. Geoexploration 15.

Henkel, H., Hult, K., Eriksson. L., and Johansson, L., 1983: Neotectonics in northern Sweden - Geophysical investigations. SKBF/KBS Teknisk Rapport 83-57.

Henkel, H., 1988: SKB projekt bergets stabilitet. Tektoniska studier vid Lansjärv. Dokumentation av profiler över olika exempel på tektoniskt-morfologiska strukturer i undersökn.området 25-27 K - N. SKB AR 88-07.

Henkel, H., and Wållberg, B., 1988: The post-glacial faults at Lansjärv. Ground geophysical measurements and interpretations in a 40 x 20 km surrounding area. SKB AR 88-05.

Kerrich, R., 1986: Fluid infiltration in fault zones: Chemical, isotopic and mechanical effects. PAGEOPH 124 Pt 1-2, pp 226-268.

Kovacs, L.C., Berero, C., Johnson, G.L., Pilger, R.H., Taylor, P.T., and Vogt, P.R., 1986: Residual magnetic anomaly chart of the Arctic Ocean region. US Naval Res. Lab. and Naval Ocean Res. and Development Activity.

Kresten, P., and Printzlau, I., et al., 1977: New ages of carbonatitic and alcaline ultramafic rocks from Sweden and Finland. GFF 99 pp 62-65.

Kujansuu, R., 1972: On landslides in Finnish Lapland. Geol. Survey Finland Bull. 256, pp 1-22.

Lagerbäck, R., 1979: Neotectonic structures in northern Sweden. GFF 100 pp 263-269.

Lagerbäck, R., and Witschard, F., 1983: Neotectonics in northern Sweden-Geological investigations. SKBF/KBS Teknisk Rapport 83-58.

Schack Pedersen, S.A., and Håkansson, E., 1987: Structural styles of the Wandel Hav strike-slip mobile belt. In: Abstracts of the 18th Nordic Geological Meeting - Geological Survey of Denmark, ISBN 87-88640-07-08.

Sharp, R.V., 1979: Implications of surficial strike-slip fault patterns for simplification and widening with depth. In Proceedings of Conference VIII Analysis of fault zones in bedrock. US Geological Survey Open File Report 79-1239.

Sibson, R.H., 1977: Fault rocks and fault mechanisms. Journ Geol Soc London 133 pp 191-213.

Sibson, R.H., 1986: Brecciation process in fault zones: Interference from earthquake rupturing. PAGEOPH 124 Pt 1-2 pp 159-176.

SKB, 1986: Kärnkraftavfallets behandling och slutförvaring, del III Forskningsprogram 1987-1992.

Stephansson, O., 1987: Modelling of crustal rock mechanics for radio-active waste storage in Fennoscandia - Problem definition. SKB TR 87-M.

Sundh, M., and Wahlroos, J.E., 1988: SKB projekt bergets stabilitet - Tektoniska studier i Lansjärv. Dokumentation av hälltolkning och fotogrammetriska avvägningar av högsta kustlinjen. SKB AR 88-06.

Talbot, Chr., 1986: A preliminary structural analysis of pattern of post-glacial faults in northern Sweden. SKB Technical Report 86-20.

Wallace, R.E., and Morris, H.T., 1979: Characteristics of faults and shear zones as seen in mines at depth as much as 2.5 km below the surface. In: Proceedings of Conference VIII Analysis of fault zones in bedrock. US Geological Survey Open File Report 79-1239.

Wallace, R.E., and Morris, H.T., 1986: Characteristics of faults and shear zones in deep mines. PAGEOPH 124 No 1-2 pp 107-125.

List of SKB reports

Annual Reports

1977–78
TR 121
KBS Technical Reports 1 – 120.
Summaries. Stockholm, May 1979.

1979
TR 79–28
The KBS Annual Report 1979.
KBS Technical Reports 79-01 – 79-27.
Summaries. Stockholm, March 1980.

1980
TR 80–26
The KBS Annual Report 1980.
KBS Technical Reports 80-01 – 80-25.
Summaries. Stockholm, March 1981.

1981
TR 81–17
The KBS Annual Report 1981.
KBS Technical Reports 81-01 – 81-16.
Summaries. Stockholm, April 1982.

1982
TR 82–28
The KBS Annual Report 1982.
KBS Technical Reports 82-01 – 82-27.
Summaries. Stockholm, July 1983.

1983
TR 83–77
The KBS Annual Report 1983.
KBS Technical Reports 83-01 – 83-76
Summaries. Stockholm, June 1984.

1984
TR 85–01
Annual Research and Development Report 1984
Including Summaries of Technical Reports Issued during 1984. (Technical Reports 84-01– 84-19)
Stockholm June 1985.

1985
TR 85-20
Annual Research and Development Report 1985
Including Summaries of Technical Reports Issued during 1985. (Technical Reports 85-01-85-19)
Stockholm May 1986.

1986
TR 86-31
SKB Annual Report 1986
Including Summaries of Technical Reports Issued during 1986
Stockholm, May 1987

1987
TR 87-33
SKB Annual Report 1987
Including Summaries of Technical Reports Issued during 1987
Stockholm, May 1988

Technical Reports

1988
TR 88-01
Preliminary investigations of deep ground water microbiology in Swedish granitic rocks
Karsten Pedersen
University of Göteborg
December 1987

TR 88-02
Migration of the fission products strontium, technetium, iodine, cesium and the actinides neptunium, plutonium, americium in granitic rock
Thomas Ittner[1], Börje Torstenfelt[1], Bert Allard[2]
[1]Chalmers University of Technology
[2]University of Linköping
January 1988

TR 88-03
Flow and solute transport in a single fracture. A two-dimensional statistical model
Luis Moreno[1], Yvonne Tsang[2], Chin Fu Tsang[2], Ivars Neretnieks[1]
[1]Royal Institute of Technology, Stockholm, Sweden
[2]Lawrence Berkeley Laboratory, Berkeley, CA, USA
January 1988

TR 88-04
Ion binding by humic and fulvic acids: A computational procedure based on functional site heterogeneity and the physical chemistry of polyelectrolyte solutions
J A Marinsky, M M Reddy, J Ephraim, A Mathuthu
US Geological Survey, Lakewood, CA, USA
Linköping University, Linköping
State University of New York at Buffalo, Buffalo, NY, USA
April 1987

TR 88-05
Description of geophysical data on the SKB database GEOTAB
Stefan Sehlstedt
Swedish Geological Co, Luleå
February 1988

TR 88-06

Description of geological data in SKBs database GEOTAB

Tomas Stark
Swedish Geological Co, Luleå
April 1988

PLATE 1

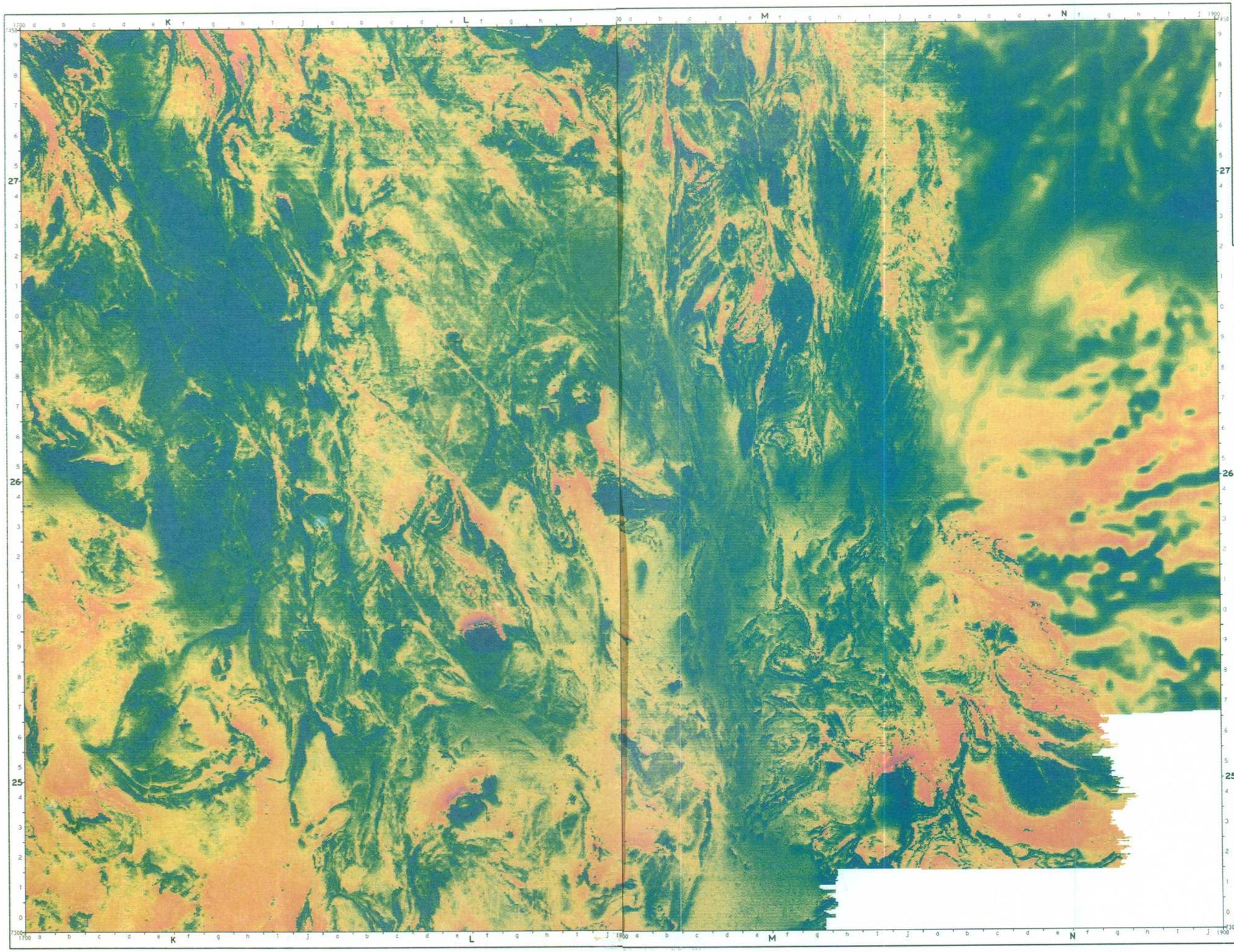

FLYGMAGNETISK KARTA
AEROMAGNETIC MAP
25-27 M-N

0.0 SKALA 1:250 000 12.5 Km

Magnetiskt restdualfält
Magnetic residual field

Referensfält: DGRF(1965.0)
Reference field: DGRF(1965.0)

Anomali
Anomaly
NANOTESLA (nT)
3000
1800
600
0
-600
-1800
-3000

Referensfält samt flygriktning inom kartorgan
Reference field and flight direction within map area

51800
51700
51600
51500

Flygriktning
Flight direction:
Referensfält:
Reference field:

200-METERSPUNKTER

Indexkarta
Index map

SVERIGES GEOLOGISKA UNDERSÖKNING

19870416

PLATE 2

TYNGDKRAFTSKARTA
GRAVITY MAP
25-27 M.N

Bouguer anomali
Bouguer anomaly

SKALA
SCALE 1:250000

0 2 4 6 8 10 km

Bouguer anomaly values in Finland are extracted from the 2.5 km grid of the Nordkalott project increased by 9.7 mgal to compensate for the differences between the reference systems.

9.0
8.0
7.0
6.0
5.0
4.0
3.0
2.0
1.0
0.0
-1.0
-2.0
-3.0
-4.0
-5.0
-6.0
-7.0
-8.0
-9.0
-10.0
-11.0
-12.0
-13.0
-14.0
-15.0
-16.0
-17.0
-18.0
-19.0
-20.0
-21.0
-22.0
-23.0
-24.0
-25.0
-26.0
-27.0
-28.0
-29.0
-30.0
-31.0
-32.0
-33.0
-34.0
-35.0
-36.0
-37.0
-38.0
-39.0
-40.0

Referenssystem Reference system	
Kalibreringssystemet Calibration system	: ECS 62
Höjdsystem Elevation system	: 1970
Internationella formeln International formula	: 1930
Bouguer-densitet Bouguer-density	: 2.67 g/cm³
Uppmätt Measured	:
Genomsnittligt mätpunktsavstånd Mean station spacing	:
Terrängkorrection inom Terrain correction within	: 12.5 km
Genomsnittligt fel Mean error	: 0.2 mgal
Ekvidistans Contour interval	: 1.0 mgal

SVERIGES GEOLOGISKA UNDERSÖKNING

870325

HÖJDKARTA
ELEVATION MAP
25-27 M-N

Höjd över havet
Altitudes above sea level

SKALA
SCALE 1:250000

0 2 4 6 8 10 km

Höjder
Altitudes

Enhet
Units = Meter

Above	585.00
570.00 –	585.00
555.00 –	570.00
540.00 –	555.00
525.00 –	540.00
510.00 –	525.00
495.00 –	510.00
480.00 –	495.00
465.00 –	480.00
450.00 –	465.00
435.00 –	450.00
420.00 –	435.00
405.00 –	420.00
390.00 –	405.00
375.00 –	390.00
360.00 –	375.00
345.00 –	360.00
330.00 –	345.00
315.00 –	330.00
300.00 –	315.00
285.00 –	300.00
270.00 –	285.00
255.00 –	270.00
240.00 –	255.00
225.00 –	240.00
210.00 –	225.00
195.00 –	210.00
180.00 –	195.00
165.00 –	180.00
150.00 –	165.00
135.00 –	150.00
120.00 –	135.00
105.00 –	120.00
90.00 –	105.00
75.00 –	90.00
60.00 –	75.00
45.00 –	60.00
30.00 –	45.00
15.00 –	30.00
0.15 –	15.00
Below	0.15

SVERIGES GEOLOGISKA UNDERSÖKNING

870512

PLATE 4

ELEVATION RELIEF MAP

0 20 km

27

26

25

K L M N

LANTMÄTERIVERKET

PLATE 5

BERGGRUNDSKARTA

GEOLOGICAL MAP

25–27/M–N

Skala 1:250 000

0 5 0 10 15 20 km

DOMINERANDE BERGART I HÄLL

- Granit, pegmatit, aplit
- Monzonit, syenit
- Granodiorit, kvartsdiorit, diorit
- Gabbro
- Granitoid gnejs
- Mafisk vulkanit, amfibolit
- Felsisk vulkanit, porfyr, leptit
- Kvartsit, kvarsitisk gnejs
- Glimmerskiffer, glimmergnejs
- Kalksten, dolomit
- Suprakrustalgnejs (odifferentierad)

STRATIGRAFI

SENOROGENA SVECOKARELSKA INTRUSIV (1750–1800 Ma)

- Linagranit, migmatitgranit

INTRAOROGENA INTRUSIV

- Gabbro
- Monzonit
- Granit

ÖVRE SUPRAKRUSTALEN

- Svartlågruppen (kvartsit, skiffer, amfibolit)
- Balingeporfyrit

PRIMOROGENA SVECOKARELSKA INTRUSIV (1850–1900 Ma)

- Gabbro–diorit
- Diorit–granodiorit

MELLERSTA SUPRAKRUSTALEN

- Kiruna–Arvidsjaurskomplexet (Porfyrgruppen) (mafiska vulkaniter/felsiska vulkaniter, vulkaniklastiska metasediment)
- Råneågruppen (skiffer–migmatit, metagråvackor/amfibolit)

UNDRE SUPRAKRUSTALEN

- Kalix grönstensgrupp (grönsten, amfibolit/kalksten, dolomit)
- Sockbergetgruppen (kvartsit, fsp–kvartsrisk gnejs, amfibolit, odiff./amfibolit)

- Lagrad gabbro (2450 Ma)

UNDERSTA SUPRAKRUSTALEN

- Korpilombologruppen

UNDERLAGET, >2800 Ma

- Granitgnejskomplexet

- Migmatit (senorogen granitisering)
- Inneslutning (xenolit)
- Diabas
- Häll eller hällområde
- Mindre häll eller hällområde
- Magnetiska konnektioner
- Förkastning
- Regional stryknin/stupning (lagring, dominerande foliation)
  - 0–10 grader
  - 15–30 "
  - 35–55 "
  - 60–75 "
  - 80–90 "

SVERIGES GEOLOGISKA UNDERSÖKNING

Kartan framställd med CAMPUS-systemet vid ADB-sektionen, SGU.

PLATE 6

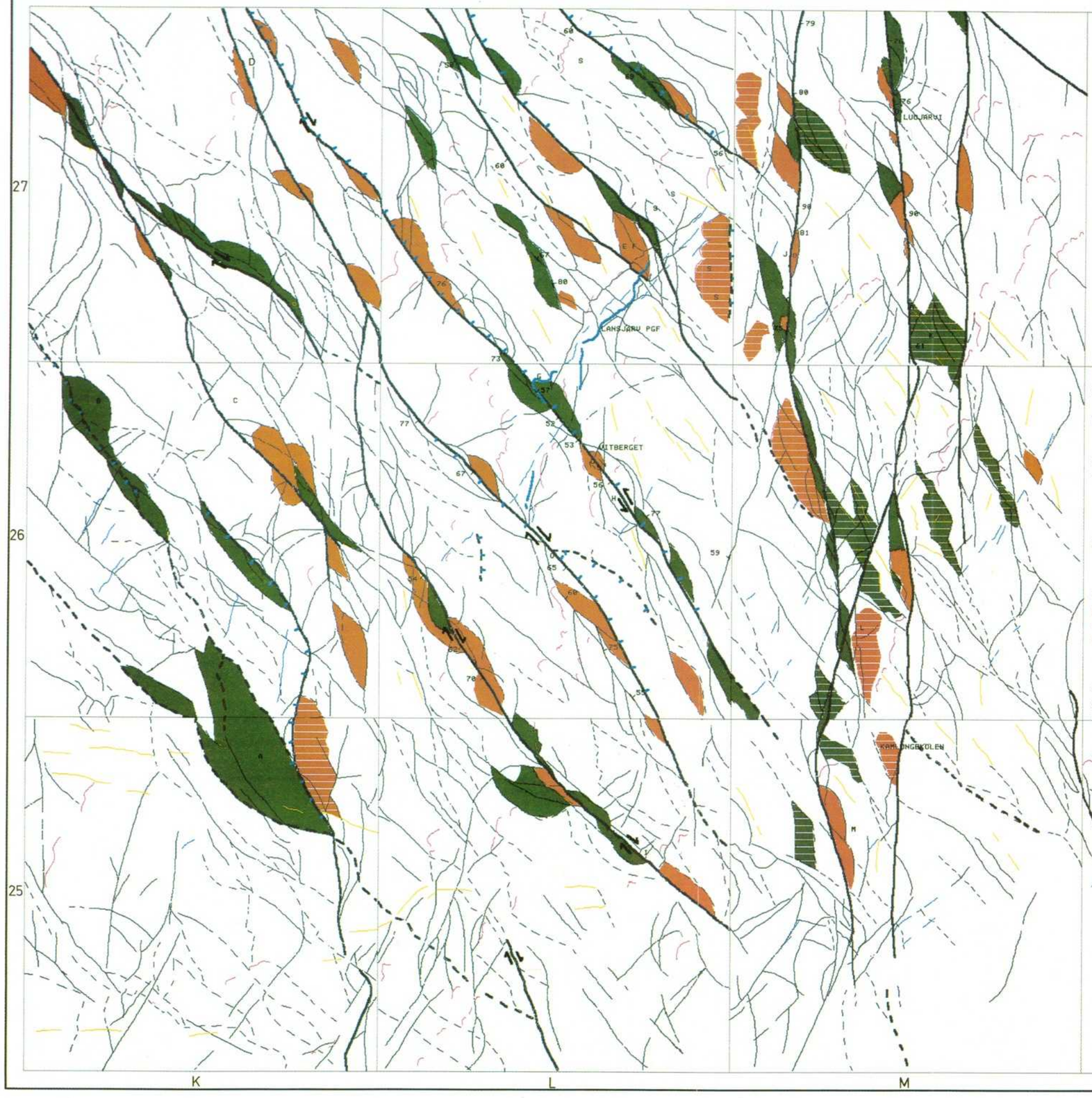

TECTONIC INTERPRETATION MAP

25 - 27 K - N SCALE 1:250 000 0 10 KM

LINEAMENTS

AEROMAGNETICALLY INDICATED STEEP SHEAR ZONES AND FAULTS

WIDTH APPROX 200 M — LESS WIDE

MORPHOLOGICALLY INDICATED FAULT ZONES

STEEP DIP — WIDE - - - SMALL

SHALLOW DIP — APPARENT IN TOPOGRAPHIC RELIEF

POST-GLACIAL FAULT SCARPS

KNOWN — SUSPECTED

BLOCK MOVEMENTS

LATERAL MOVEMENTS

WITH RESPECT TO PRECAMBRIAN REFERENCE STRUCTURES

WITH RESPECT TO MORPHOLOGY

VERTICAL MOVEMENTS

WITH RESPECT TO TERRAIN ELEVATION (BARBS ON LOWER BLOCK)

MORPHOLOGICALLY INDICATED SMALLER SHEAR LENSES ASSOCIATED TO MAJOR FAULT ZONES

POSITIVE NEGATIVE

OTHER MORPHOLOGIC FEATURES INDICATIVE OF BLOCK MOVEMENTS

POSITIVE NEGATIVE

SUSPECTED POST-GLACIAL SHEAR LENSES

LAND SLIDES

ORIENTATION OF STRUCTURES

65 MAGNETICALLY CALCULATED DIP OF STEEP FAULT ZONES

REFERENCE TO TEXT FOR PROFILES

A ... N

THIS INTERPRETATION IS BASED ON A COMBINED DIGITAL ANALYSIS OF AEROMAGNETIC (200 X 200 M) , TERRAIN ELEVATION (100 X 100 M) , TERRAIN RELIEF AND GRAVITY (400 X 400 M) DATA. THE MAP WAS CONSTRUCTED WITH THE IMAGE ANALYZING SYSTEM EBBA II.

S G U
GEOLOGICAL SURVEY OF SWEDEN
HERBERT HENKEL 87 06 30